MICHIGAN STATE UNIVERSITY

CYCLOTRON LABORATORY

NUCLEAR LIQUID-GAS PHASE TRANSITION AND FRAGMENT PRODUCTION IN HEAVY-ION COLLISIONS

LASZLO P. CSERNAI

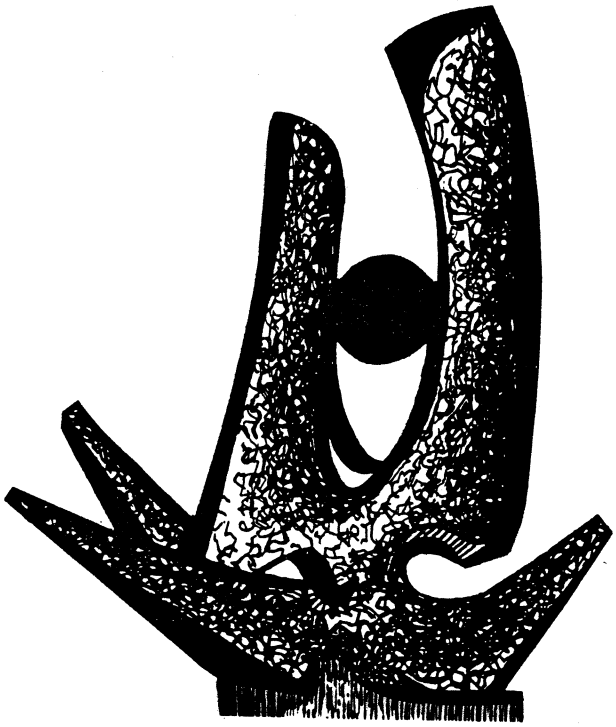

DECEMBER 1986

MSUCL-587

MSUCL - 587

NUCLEAR LIQUID-GAS PHASE TRANSITION

AND

FRAGMENT PRODUCTION IN HEAVY-ION COLLISIONS

Laszlo P. Csernai[†]
National Superconducting Cyclotron Laboratory
Michigan State University
East Lansing, Michigan 48824-1321 USA

Invited Lectures
at the

Workshop on High Energy Heavy Ion Collisions and
Quark Degrees of Freedom in Nuclei
Puri, INDIA, January 2-15, 1987

December, 1986

[†]On leave from the Central Research Institute for Physics, Budapest, Hungary. This work was supported by the National Science Foundation under grant no. PHY-86-11210

TABLE OF CONTENTS

END OF TABLE

1. The nuclear equation of state

1.1 General Considerations

From conventional nuclear physics we know that there is a stable equilibrium state at the normal nuclear density n_o=0.145-0.17 fm^{-3} [My76, Be71] with a compressibility of K=180-240 MeV [BG76] and a binding energy of 16 MeV/nucleon. If we want to learn about the equation of state (EOS) at other densities and higher temperatures we have to rely mostly on theoretical estimates. The high density high temperature part of the equation of state is decisive in the first, compression stage of the collision. The low density behavior of nuclear matter determines the observables and the reaction mechanism of the final expansion stage in a collision before the breakup.

In this lecture we will concentrate on the low density part of the nuclear equation of state, which is directly related to the final fragmentation.

After an energetic nucleus-nucleus collision, many light nuclear fragments, a few heavy fragments and a few mesons (mainly pions) are observed in the 100 MeV - 4 GeV/nucleon beam energy region. Thus the initial kinetic energy of the projectile leads to the destruction of the ground state nuclear matter and converts it into a dilute gas ($n<<n_o$) of fragments, which then loses thermal contact during the breakup or freeze-out stage. These frozen-out fragments and their momentum distributions can be measured by the detectors considering also the fact that some excited fragments can decay while reaching the detectors.

In early theoretical studies it was assumed that the observed fragments formed an ideal gas mixture at the breakup. [WG76,Me77, etc.]. This approximation seemed to be quite applicable at higher energy collisions E>1GeV/nucleon but at lower energies the numbers of composite fragments deviated from the theoretical predictions.

It was realized that the ideal gas approach is too crude when many composites are present. As a first approximation the volumina of the composite particles were taken into account in statistical models [SC81, FR82, CK86b, SB83]. This simulation of repulsive interactions made the models more accurate at higher densities around n_o, but it was not sufficient to yield a first order phase transition [CF87].

It should be realized that the finite volume effect, as well as the compressional part of the equation state, is a consequence of nuclear interactions. To treat both repulsive and attractive interactions in a consistent manner the nuclear matter and the mixture of nucleons and deuterons were considered in quantum many body theory [RM82]. This work was later extended to more light clusters, and it was shown that it leads to a first order phase transition with a critical temperature of T_c=20.3 MeV at n_c = 0.07 fm^{-3} [RS83]. A further improvement by including Coulomb effects [RS83] leads to a fragment distribution differing from the law of mass action used in early models. Jagaman et al. [JM84] considered also the effects of the finite size of a nuclear system and found that if A decreases from A=200 to 50 the critical temperature T_c drops from 19.1 MeV to 16.5 MeV. The inclusion of Coulomb interaction decreases these values further to 15.7 and 15.5 MeV respectively. The density at the critical point was found to be n_c=0.054-0.065fm^{-3}.

1.2 A simplified equation of state

Considering the major properties of the nuclear equation of state for densities below n_o the theories converge: a liquid gas phase transition is clearly predicted with T_c=15-20 MeV and n_c=0.3-0.5 n_o. More accurate information and further details can be obtained only from thorough experimental research and comparison of experimental and theoretical results. Before we discuss the properties of the nuclear equation of state let us introduce the general notation of thermodynamic variables (Table 1). If we have defined one of the "state functions" or

"thermodynamical potentials" in terms of its proper variables like $e(s,n)$, $F(T,V,N)$ or $\mu(T,p)$ all others thermodynamical variables can be obtained by differentiating the thermodynamical potential. For example: The equation of state $p=p(T,n)$ can be obtained from the Helmholtz free energy density as $p(T,n)=n.f_{,n}-f$. (The comma denotes the partial derivative: $a_{,x}= \partial a/\partial x$.)

Table 1

THERMODYNAMICAL VARIABLES

V=volume	$\nu=V/N$	$n=N/V$
N=particle number	$\sigma=S/N$	$s=S/V$
S=entropy		
Extensives	Specific Extensives (1/N)	Extensive densities (1/V)
$E(S,V,N)=TS-pV+\mu N$	$\varepsilon(\sigma,\nu)=T\sigma-p\nu+\mu$	$e(s,n)=Ts-p+\mu n$
$dE=TdS-pdV+\mu dN$	$d\varepsilon=Td\sigma-pd\mu$	$de=Tds+\mu dn$
		eg.: $p=e-se_{,s}-ne_{,n}$
One intensive:		
Enthalpy:		
$H(S,p,N)=E+pV=TS+\mu N$	$\chi(\sigma,p)=\varepsilon+p\nu=T\sigma+\mu$	$w(s,n)=e+p=Ts+\mu n$
$dH=TdS+Vdp+\mu dN$	$d\chi=Td\sigma+\nu dp$	$dw=Tds+\mu dn$
		(redundant)
Helmholtz free energy:		
$F(T,V,N)=E-TS=\mu N-pV$	$\phi(T,\nu)=\varepsilon-T\sigma=\mu-p\nu$	$f(T,n)=e-Ts=\mu n-p$
$dF=-SdT-pdV+\mu dN$	$d\phi=-\sigma dT-pd\nu$	$df=-sdT+\mu dn$
$X(S,V,\mu)=E-\mu N=TS-pV$	_	$x(s,\mu)=e-\mu n=Ts-p$
$dX=TdS-pdV$		$dx=Tds-nd\mu$
Two intensives:		
Gibbs free energy		
$G(T,p,N)=E+pV-TS=\mu N$	$\mu(T,p)=\varepsilon-T\sigma+p\nu$	-
$dG=-SdT+Vdp+\mu dN$	$d\mu=-\sigma dT+\nu dp$	
$\Omega(T,V,\mu)=-pV=E-TS-\mu N$	-	$z(\mu,T)=-p=e-Ts-\mu n$
$d\Omega=-SdT-pdV-Nd\mu$		$dz=-sdT-nd\mu$
$Y(S,p,\mu)=TS=E+pV-\mu N$	-	-
$dY=TdS+Vdp-Nd\mu$		
Gibbs-Duhem relation:		
$E+PV-TS-\mu N=0$	$d\mu=-\sigma dT+\nu dp$	$dp=sdT+nd\mu$
$-SdT+Vdp-Nd\mu=0$		

As an example which is used in the majority of the literature [SB83, SN80, CB80,CS83, Da79, GK84, Ka84, Ni79, MS83], let us define an analytic parametrization for the nuclear equation of state. The thermodynamical potential e=e(n,s) as a function of baryon density n, and entropy density s is given by:

$$e(n,s) = e_o(n) + e^*_{FG}(n,s) - e^*_{FG}(n,0) \ , \qquad (1.1)$$

where $e_o(n)$ is the ground state energy density, and $e^*_{FG}(n,s)$ is the energy density of an ideal Fermi-gas. We can parametrize the ground state energy density as [Ka84]

$$e_o(n) = n_o \sum_{i=2}^{5} a_i \left(\frac{n}{n_o}\right)^{i/3+1} \ , \qquad (1.2)$$

where a=+21.1, -38.3, -26.7, +35.9 MeV for i=2,....5 respectively. This parametrization yields a binding energy $\varepsilon_o(n_o)=e_o(n_o)/n_o$ = -8MeV (instead of -16 to simulate finite size effects) and a nuclear compressibility K=210MeV at $n_o=0.15 fm^{-3}$. Note that this parametrization is used for small nuclear densities $n<2n_o$. At high densities the sound speed exceeds the speed of light. For the thermal part of the energy density we use the nonrelativistic ideal Fermi-gas approximation because for the low density and temperature at the breakup relativistic corrections are negligible. Then the energy density e^*_{FG} depends on the density n and specific entropy $\sigma=s/n$ as [LL54]:

$$e^*_{FG}(n,s) = \left(\frac{n}{m}\right)^{5/3} y(\sigma) \qquad (1.3)$$

where y is a dimensionless quantity and it depends on the specific entropy σ (or μ/T) which is also dimensionless. $y(\sigma)$ can be given in integral form [LL54], but in actual calculations usually practical analytic parametrizations are used [Ka84, CK86].

Other thermodynamical quantities can then be calculated from standard thermodynamic relations:

$$T(n,s)=e_{,s} = \frac{n^{2/3}}{m}\, y'(\sigma) \quad , \tag{1.4}$$

$$\mu(n,s)=e_{,n} = \frac{1}{3}\sum_{i=2}^{5}(i+3)a_i\left(\frac{n}{n_o}\right)^{i/3} + \frac{5}{3}\frac{e^{*}_{FG}}{n} - T\sigma \quad , \tag{1.5}$$

$$p(n,s) = p_o(n) + \frac{2}{3}\, e^{*}_{FG}\,(n,s) \quad , \tag{1.6}$$

where

$$p_o(n) = \frac{n}{3}\sigma \sum_{i=2}^{5} i a_i \left(\frac{n}{n_o}\right)^{i/3+1} \quad .$$

The equation of state represents a stable equilibrium configuration only if the energy has a minimum. This condition is satisfied if the matrix $M_{ik} = e_{,ik}$ (where k,i = n,s) is positive definite. This requirement leads to two independent constraints on the derivatives of the thermodynamical parameters [LL54, Section 21]:

$$c_v = T\, s(T,v)_{,T} \quad >0 \tag{1.7}$$

$$\kappa_T = -\frac{1}{v}\, v(p,T)_{,p} \quad >0 \tag{1.8}$$

where κ_T is the isothermal compressibility, and c_v is the isochoric specific heat. In nuclear physics the compressibility is customarily characterized by another quantity:

$$K_\sigma = 9p(\sigma,n)_{,n} \text{ and } K_T = 9p(T,n)_{,n}$$

The values quoted for the nuclear compressibility earlier are corresponding to this latter parameter: $K_0 \approx$ 180-240 MeV.

These two constraints lead to numerous other thermodynamical inequalities, which all are satisfied if eqs. (1.7-8) are. Our equation of state satisfies eq. (1.7). We, however, have to discuss the consequences of the requirement eq. (1.8). It has an implication on the isothermal sound speed v_T: $v_T^2 > 0$, i.e.

$$v_T^2 = \frac{1}{m} p(T,n)_{,n} = - \frac{\nu^2}{m} p(T,\nu)_{,\nu} = \frac{\nu^3}{m} \kappa_T^{-1} > 0 \quad . \tag{1.9}$$

If this requirement is satisfied then the adiabatic sound speed is already automatically positive because

$$v_\sigma^2 = (c_p/c_\nu) v_T^2 > v_T^2 > 0 \quad . \tag{1.10}$$

In relativistic physics the definition of sound velocities u_T, u_σ are different. Nevertheless, as it was shown in ref.[CK86] the stability requirements remain the same. Evaluating the sound velocity from the above equation of state we observe that there is a region in our thermodynamical parameter space where $u_T^2 < 0$, Fig. 1.1.

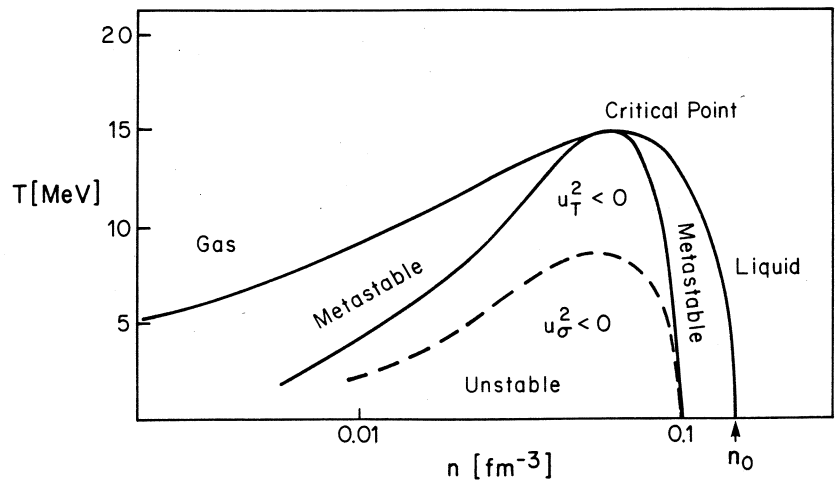

Fig 1.1 Phase diagram of the nuclear liquid gas phase transition. From [CK86].

That is, our equation of state does not represent a stable equilibrium. The region where $u_0^2 < 0$ is contained within the unstable region. There are speculations [SB83, LS84] that the matter in a relativistic heavy ion collision might penetrate into the unstable region because of rapid expansion during the collision. This is quite exciting, but these approaches have still to be justified by studies of microscopic processes using reaction rates in this unstable region.

1.3 Phase coexistence

If the temperature and density of our system falls into the unstable region, or even close to this region, it splits up into two phases. Theoretically this is also a consequence of the stability requirements. If we allow for two co-existing phases we have one more free parameter in our problem, the volume fraction of the phases i=1,2:

$$\lambda_i = V_i/V \ , \tag{1.11}$$

or equivalently the particle number fractions:

$$\alpha_i = N_i/N \ . \tag{1.12}$$

The sum of both is normalized to 1, $\alpha_1+\alpha_2 = 1$, $\lambda_1+\lambda_2 = 1$ and there is a relation among α_i, λ_i,n and $n_i = N_i/V_i$:

$$\lambda_i = \frac{n}{n_i}\ \alpha_i \qquad \text{and} \qquad \lambda_2 = \frac{n-n_1}{n_2-n_1} \ . \tag{1.13}$$

Now the requirement of the energy minimum, leads to Gibb's criteria of phase equilibrium:

$$p_1 = p_2 = p \ , \tag{1.14}$$

$$T_1 = T_2 = T \tag{1.15}$$

$$\mu_1 = \mu_2 = \mu \tag{1.16}$$

For a two phase system these requirements restrict the region of stability on the n, s plane to a line! This is the Maxwell construction line (Fig. 1.1-2), and it lies in the stable region of the previous stability study.

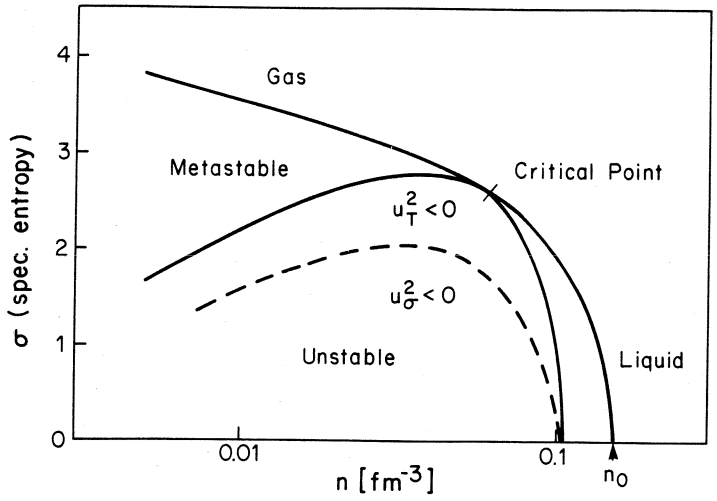

Fig. 1.2 Phase diagram on the entropy density plane. Phase equilibrium is possible above the critical entropy too!

Outside the region confined by this line the matter is stable in one single phase. Within this line but outside the $u_T^2 < 0$ region the matter is mechanically stable if formation of the other phase is hindered or delayed. The region between the Maxwell construction line and the boundary of instability $u_T^2 < 0$ is metastable: matter can be stable in this region if the other phase is not present. These are the phenomena of superheating and supercooling which are quite common in relatively slow thermodynamic processes, so we expect these phenomena to occur in relativistic heavy ion collisions.

If we solve the Gibb's criteria for our equation of state the extensive thermodynamic quantities are given along the Maxwell construction line as functions of one intensive parameter, say T. In Fig. 1.1 the density is plotted for the two phases in equilibrium n_L^{eq}

(T) and n_G^{eq} (T). The critical point at (T_c, n_c) separates the Maxwell construction line into a Liquid (L) and a Gas (G) part. The critical temperature, density and entropy density for the above equation of state (1.2) are

$$T_c = 14.9 \text{ MeV}, \qquad n_c = 0.063 \text{ fm}^{-3}, \qquad \sigma_c = 2.55.$$

If the temperature of our system is below T_c and its total density is $n_G^{eq}(T) < n < n_L^{eq}(T)$, in equilibrium the system forms a phase mixture of volume fractions λ_G and λ_L. All extensive densities, such as: s, e, w., ...etc., can be described in terms of the equilibrium parameters of the matter and the volume fractions if we neglect the surfaces separating the two phases. For specific extensives the same type of equation is valid, but with the α_G, α_L phase abundances. For example:

$$n = \lambda_G n_G^{eq}(T) + \lambda_L n_L^{eq}(T) \quad \Big| \quad \nu = \alpha_G \nu_G^{eq}(T) + \alpha_L \nu_L^{eq}(T)$$

$$e = \lambda_G e_G^{eq}(T) + \lambda_L e_L^{eq}(T) \quad \Big| \quad \varepsilon = \alpha_G \varepsilon_G^{eq}(T) + \alpha_L \varepsilon_L^{eq}(T)$$

etc.

extensive densities | specific extensives

In a heavy ion reaction in principle we might reach the phase mixture region with arbitrarily high energy collisions in the subsequent quasiadiabatic expansion [CB80] if the breakup density is sufficiently low.

Since we are interested in the final expansion stages of a heavy ion reaction when the temperature and density decrease it is imperative

to study the low temperature or low density limit of the nuclear liquid-gas phase transition. The low temperature limit of the phase transition can be discussed analytically. In this limit the thermal energy of the gas phase can be represented by the Boltzmann limit, the thermal energy of the liquid phase on the other hand by the degenerate Fermi gas limit. Similarly the compressional energy of the gas phase can be approximated by the first term of eq. (1.2) while for the liquid phase we can use a usual parametrization around the ground state:

$$e_L = \frac{K}{18}\left(\frac{n}{n_o} - 1\right)^2 n - Bn + mn + e^*_{FG}(n,s), \tag{1.17}$$

$$e_G = na_2\left(\frac{n}{n_o}\right)^{2/3} + \frac{3}{2}nT + mn \tag{1.18}$$

where $e^*_{FG}(n,s) = \frac{b^2}{4} mn^{1/3} T^2$, at low temperatures, $p_{FG} = \frac{2}{3} e_{FG}$, B=8 MeV is the binding energy, and b=1.809. From the Gibbs criteria then we obtain for the specific entropies:

$$\sigma_G^{eq}(T) = 5/2 + B/T = 5/2 - \ln\left[\frac{n}{4}G\left(\frac{2\pi}{mT}\right)^{3/2}\right] , \tag{1.19}$$

$$\sigma_L^{eq}(T) = 1/2\, b^2 m\, n_L^{eq}(T) \approx \frac{1}{2} b^2\, mn_o^{-2/3}\, T , \tag{1.20}$$

and for the densities:

$$n_G^{eq}(T) = 4(mT/2\pi)^{3/2}\, e^{-B/T} , \tag{1.21}$$

$$n_L^{eq}(T) = n_o - \frac{3}{2}\frac{b^2 mT^2}{K} n_o^{1/3} . \tag{1.22}$$

Thus the entropy of the gas phase grows to infinity as B/T if $T \to 0$. Since at low T $n_G^{eq} << n_L^{eq}$ and $n_L^{eq} \approx n_o$ the breakup temperature t_{BU} is more

characteristic than the n_{BU} of the total system. Fortunately this is also a measurable quantity and lies in the 4-14 MeV region [PC85, PC84, MB84] for a wide range of beam energies. This suggests, with the help of eq. (1.19), that we might reach the phase mixture in energetic reactions up to an initial entropy of σ_{max}^{BU} = 3-4.5. If we are above the critical entropy $\sigma_c \approx 2.5$ than this happens in the gas phase and droplet formation may occur. Below the critical entropy the phase mixture boundary is reached in the liquid phase and initially small bubbles of gas phase are formed. These possibilities, however, depend strongly on the dynamics of the whole heavy ion collision.

1.4 Critical exponents

It will be imperative to mention a few results about critical phenomena. The critical opalescence in liquid gas phase transition was observed more than a century ago and in the 1940's Guggenheim [Gu45] realized that several fluids behave similarly around the critical point of the liquid-gas phase transition. This lead to the extended study of the critical exponents which started in the 1960's. (see ref.[St71]).

Let us introduce the "order parameter" $n_L^{eq}(T) - n_G^{eq}(T)$ $(=n_L-n_G)$ and the relative deviation from the critical temperature

$$\varepsilon \approx (T-T_c)/T_c \ . \tag{1.23}$$

Guggenheim's observation was that just below the critical point

$$n_L-n_G \propto (-\varepsilon)^{\beta} \ , \tag{1.24}$$

where β is a critical exponent, which was found to be universally $\beta \approx 1/3$ for the liquids he studied. Similarly another critical exponent δ is defined at $T=T_c$ by

$$p-p_c \propto (n-n_c)^{\delta} \text{ sign } (n-n_c) \; . \qquad (1.25)$$

At the critical point the isotherm compressibility κ_T diverges or K_T tends to zero (Fig 1.3).

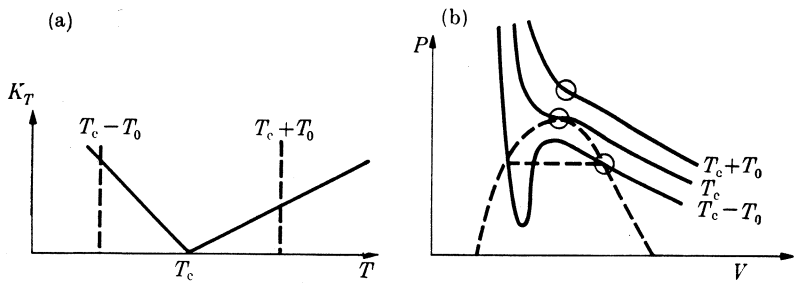

Fig. 1.3 (a) Isothermal compressibility predicted by the Van der Waals theory, $K_T=0$ at T_c. (b) three isotherms on the pV plane. The circles indicate the regions where the slope is proportional to the compressibility. From [St71].

This divergence can be parametrized by a critical exponent too:

$$\kappa_T \propto (-\varepsilon)^{-\gamma'} \; ; \; \varepsilon<0 \qquad (1.25)$$

$$\kappa_T \propto (\varepsilon)^{-\gamma} \; ; \; \varepsilon>0$$

below and above the critical point respectively. Similarly the specific heat can be parameterized around the critical point as:

$$c_v \propto (-\varepsilon)^{-\alpha'} \; ; \; \varepsilon<0 \qquad (1.27)$$

$$c_v \propto (\varepsilon)^{-\alpha} \; ; \; \varepsilon>0$$

The critical exponents can be calculated for a given equation of state. So far in nuclear physics applications, however, the critical exponents

were seldom evaluated. In Table 2 some critical exponents are listed for different models and systems

Table 2

	α $T>T_c$	α' $T<T_c$	β $T<T_c$	γ $T>T_c$	γ' $T<T_c$	σ $T=T_c$
Fluids	~0.1	~0.1	~0.34	1.35	~1	4.2
3 dim Ising model	~1/8	~1/8	~5/16	~5/4	~5/4	~5
classical mean field (Van der Waals)	0	0	1/2	1	1	3

Values of critical-point exponents for selected systems From [St71]. In [GK84] for a simple analytic equation of state the above mentioned critical exponents were evaluated and the same values were obtained as in the Van der Waals theory.

2. Dynamics of the phase transition

2.1 Stages of the heavy ion collision

The heavy-ion collision can be divided roughly into three different stages. At first the nuclear matter is compressed and heated up and a maximum compression is reached. This is the compression stage. Then the matter starts to expand adiabatically or with a relatively small dissipation ($\Delta\sigma$=10-20%) during the expansion stage. At last the system breaks up into nuclear fragments, pions, etc. If the energy is low ($E \lesssim 200$-400 MeV/nucleon) this breakup coincides with the nuclear liquid-gas phase transition providing us with the possibility to study this interesting phenomenon. At higher energies the system breaks up and freezes out much before reaching the phase transition region. let us first review briefly the models describing the first two stages of a collision based on [CK86] and then we turn to the problem of the dynamics of phase transitions in infinite systems.

In a heavy ion collision, there is a large amount of kinetic energy available, part of which will be lost during the collision due to irreversible or dissipative processes. Independent of the model we use to describe the collision, such irreversable processes are inevitable. This was realized early in the one fireball [WG76], 2-3 fireball [Da78, CG81] and firestreak [My78, GK78] models, where, without discussion of the dissipative effect, it was assumed that all available kinetic energy is thermalized at the breakup density. Given an equation of state the choice of breakup density determined the entropy increase in these models.

The assumption of global thermalization, however, is unsatisfactory as is shown for example by the collective flow. Thus more sophisticated models were developed to account for the details of the collision process. Different models assumed different grades of thermalization. One extreme is the perfect one-fluid dynamics, where immediate local thermalization is assumed. Since this model is reversible it is unable to describe a basically irreversible process. The entropy increase is

exactly zero in perfect relativistic fluid dynamics [LL53]. Therefore, no continuous solution of perfect fluid dynamics can be found which satisfies the boundary conditions in a supersonic nucleus-nucleus collision. To resolve this problem the perfect fluid dynamics should be supplemented with the relativisitic Rankine-Hugoniot relations which describe changes across a discontinuity and account for the entropy production. This model is very simple and appealing because the equation of state can be used in the solution of the fluid dynamical equations and the Rankine-Hugoniot equations give us the value of the entropy increase. Numerical perfect fluid dynamical models use the integral form of the equations, and a finite calculational grid. Thus the Rankine- Hugoniot relations are satisfied between each cell, which results in dissipation and entropy increase, or in other words in numerical viscosity.

A more realistic model is the viscous fluid dynamics where only approximate local thermalization is assumed. This model yields the shock fronts and the dissipation directly without any further assumption. However, knowledge of transport coefficients is also needed, not only the equation of state. Here dissipation or irreversibility is present because we allow heat and momentum transfer between neighboring fluid elements and allow the system to develop towards global thermalization.

If we do not require local thermalization at all, we would have to solve the relativistic transport equations. This is a very difficult task but some models, like the intranuclear cascade (INC) [Cu80, CJ83, Cu84, BC81, TG83, GI79], the two and three fluid dynamical models [AG78, CL82], molecular dynamics models (Fig. 2.1) [WY78,BP80, MH84,VJ85,AS86], transport models with mean field and Pauli principle (BUU-VUU-BN) [KJ85,BK84b,MS85,GB86] and some transport models [Ma81, Ma84, Ma84b] yield reasonable approximate solutions. Since entropy can be defined for nonequilibrated systems the dissipation and entropy increase can be evaluated [BC81,GT85] in these models. This is in spite of the fact that equilibrium and near equilibrium thermodynamics cannot be applied,

nor can the nonequilibrium system be represented by an equation of state.

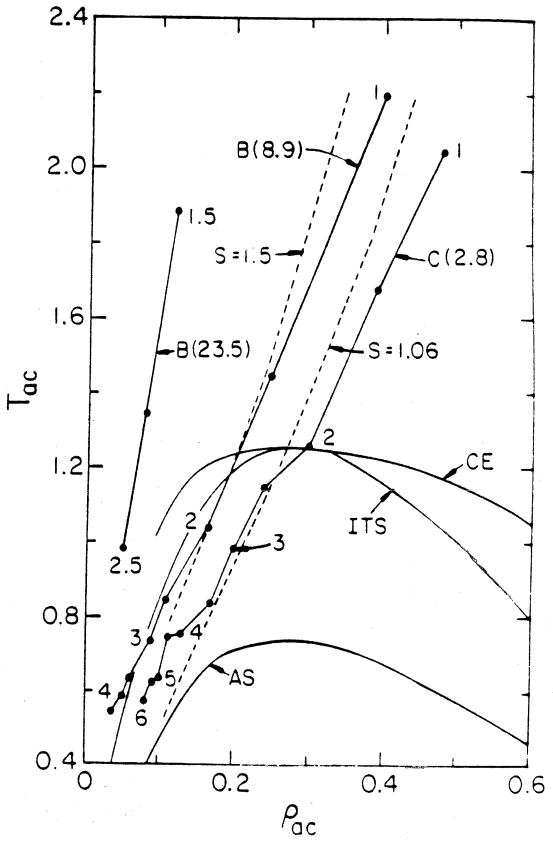

Fig. 2.1 Dynamical path calculated in a molecular dynamical model across the liquid gas phase transition region. Compared to the adiabatic expansion path (dashed lines) there is an observable entropy increase, especially in the vicinity of the adiabatic spinodal AS where $u_0^2=0$. From [VJ85].

In these cases irreversibility or dissipation occurs because of processes driving the system to some kind of equilibrium not present originally in the system. There is one more source of entropy increase which may appear both in the compression and expansion stages of a collision if a phase transition is present. The phase equilibration may not be instantaneous, and a delay in the equilibration leads to dissipation also. The nonequilibrium phase transition in a dynamical system always means that Gibb's criteria (1.14-16) for the phase equilibrium are not satisfied. This can happen in two ways. One is superheating or supercooling when the new phase does not appear for a while and the system expands into a thermodynamical state in the metastable (or unstable) region. The other possibility is that the new phase appears but not in sufficient amount to reach the phase

equilibrium. The dynamical phase transition can happen in phase equilibrium, with or without dissipation. In this case Gibb's criteria are always satisfied. This is possible if the microscopic reactions restoring phase equilibrium are faster than the speed of the expansion.

2.2 Dynamics of Nonequilibrium Phase Transitions

Dissipation and irreversibility may arise from phase transitions in a dynamical system. If the system has the possibility of forming two different phases there is always an optimum particle number $-(\alpha_i)$ or volume $-(\lambda_i)$ ratio of the phases which corresponds to the energy minimum or entropy maximum. In a rapidly changing system with finite reaction rates the system may never reach this equilibrium configuration and thus a dissipative nonequilibium process ensues.

To reach a metastable or even an unstable region having one single phase in a rapid dynamical expansion is not impossible because the perturbations restoring equilibrium develop as

$$e^{i(px-\omega t)} = e^{2\pi i(x/\lambda - t/\tau)} \sim e^{i2\pi x/\lambda}\, e^{-i2\pi ut/\lambda}$$

If u is imaginary this gives rise to a growing fluctuation - rising with the time scale $\tau = \lambda/u$. At the boundary $u_0^2 = 0$, $u_T^2 \approx -0.006c^2$. So isothermal fluctuations of the size of $\lambda \approx 5$fm may develop in 60 fm/c. This is somewhat longer than a typical reaction time.

Let us discuss the dissipation in a dynamical first order phase transition in general terms. Assume that the system is thermalized but the Gibbs criteria are not necessarily fulfilled. The volume average of the energy momentum tensor in a small local volume element containing both phases can be written as

$$T^{\mu\nu} = \sum_r \lambda_r T_r^{\mu\nu}; \qquad (2.1)$$

where $T_r^{\mu\nu} = (e+p)_r u^\mu u^\nu - p_r g^{\mu\nu}$ and r=L,G. Let us derive the entropy production in such a mixture in a manner similar to [LL53, Section 126]. From

$$T^{\mu\nu}{}_{,\nu} u_\mu = 0 \quad , \tag{2.2}$$

inserting the form (2.1) of the energy momentum tensor

$$\sum_r \left[\lambda_r (w_r u^\mu u^\nu - p_r g^{\mu\nu})\right]_{,\nu} u_\mu = 0 \quad , \tag{2.3}$$

we obtain:

$$\sum_r [(\lambda_r w_r u^\nu)_{,\nu} \underbrace{u^\mu u_\mu}_{=1} + \lambda_r w_r \underbrace{u^\nu u_\mu}_{=0} u^\mu{}_{,\nu} - u^\nu (\lambda_r p_r)_{,\nu}] = 0 \ , \tag{2.4}$$

which thus reduces to:

$$\sum_r (\lambda_r w_r u^\mu)_{,\mu} - u^\mu (\lambda_r p_r)_{,\mu} = 0 \tag{2.5}$$

Performing the derivations

$$\sum_r u^\mu (\lambda_r w_r)_{,\mu} + \lambda_r w_r u^\mu{}_{,\mu} - u^\mu (\lambda_r p_r)_{,\mu} = 0 \ , \tag{2.6}$$

and using the continuity equaton $(nu^\mu)_{,\mu}=0$ which implies that $u^\mu{}_{,\mu} = -(n_{,\mu}/n)\ u^\mu$ eq. (2.6) can be written as

$$\sum_r nu^\mu [\underbrace{\tfrac{1}{n}(\lambda_r w_r)_{,\mu} - \tfrac{1}{n^2} n_{,\mu}\ \lambda_r w_r}_{(\lambda_r w_r/n)_{,\mu}} - \underbrace{\tfrac{1}{n}(\lambda_r p_r)_{,\mu}}_{\lambda_r p_{r,\mu} + p_r \lambda_{r,\mu}}] = 0 \ . \tag{2.7}$$

Using the relation between the volume and particle number ratios of the two phases $\lambda_r=(n/n_r)\alpha_r$, which follows from the definition (1.11-12) we arrive at

$$\sum_r nu^\mu[(\alpha_r w_r/n_r)_{,\mu} - \frac{\alpha}{n_r}\, p_{r,\mu} - p_r/n\ \left(\frac{n\,\alpha_r}{n_r}\right)_{,\mu}]=0\ , \tag{2.8}$$

and after performing the differentiations we get

$$\sum_r nu^\mu[\ \alpha_{r,\mu}\left(\frac{w}{n}_r\right) + \alpha_r\left(\frac{w}{n}_r\right)_{,\mu} - \frac{\alpha}{n}_r\, p_{r,\mu} - \frac{p}{n}_r\left(\frac{n\alpha}{n}_r\right)_{,\mu}]=0\ . \tag{2.9}$$

Now we should makes use of the thermodynamical relations (see Table 1) $\chi_r = w_r/n_r = \varepsilon_r+p_r\nu_r=T_r\sigma_r+\mu_r$, $d\chi=Td\sigma-\nu dp$, and so $T_r d\sigma_r=d\left(\frac{w}{n}r\right)-\frac{1}{n_r}dp_r$, and we can write eq. (2.9) in the form

$$n\sum_r \dot{\alpha}_r(T_r\sigma_r+\mu_r) +\alpha_r\, T_r\, \dot{\sigma}_r - p_r/n\ (n\alpha_r/n_r)^{\bullet} = 0\ , \tag{2.10}$$

where $^{\bullet}$ is the derivative with respect to the proper time $(\partial/\partial T)$ or $\dot{a}= u^\mu a_{,\mu}$. Reorganizing the terms we arrive at:

$$n\sum_r T_r(\dot{\alpha}_r\sigma_r+\alpha_r\dot{\sigma}_r) + \dot{\alpha}_r\mu_r - p_r\nu\ \dot{\lambda}_r= \tag{2.11}$$

$$= n\sum_r(\alpha_r\sigma_r)^{\bullet}T_r +\dot{\alpha}_r\mu_r - p_r\nu\ \dot{\lambda}_r= 0$$

Let us now assume that $T_G=T_L$ i.e. thermal equilibrium is established (but the two other Gibb's criteria are not satisfied):

$$T\ (\ \Sigma_r\alpha_r\sigma_r)^{\bullet} = -\ \Sigma_r\dot{\alpha}_r\mu_r + \nu\ \Sigma_r p_r\dot{\lambda}_r\ . \tag{2.12}$$

Expressing the total entropy production our final result is

$$\dot{\sigma} = -\frac{1}{T}(\mu_1-\mu_2)\,\dot{\alpha}_1+\frac{\nu}{T}(p_1-p_2)\,\dot{\lambda}_1 \ . \qquad (2.13)$$

Thus nonequilibrium phase transition leads to entropy increase! To solve the complete dynamical problem each of the not satisfied Gibbs criteria should be replaced by a dynamical equation. According to nonequilibrium thermodynamics the generalized currents like $\dot{\alpha}_r$ or $\dot{\lambda}_r$ are driven by generalized thermodynamical forces which act in the direction of restoring the equilibrium:

$$\mu_1=\mu_2 \quad \text{--> } \dot{\alpha}_1 = -(\alpha-\alpha_{eq}(n,T,p))/\tau_{ch} \qquad (2.14)$$

$$p_1=p_2 \quad \text{--> } \dot{\lambda}_1 = -(\lambda-\lambda_{eq}(n,T,p))/\tau_{pr} \ . \qquad (2.15)$$

Consequently the dissipation is determined by the ratio of the time scale characterizing the dynamics of the process τ_{dyn}, and the equilibration time τ_{ch} and τ_{pr}.

The question of finite size systems will be discussed in section 3. If, however, a phase transition is sensible for small systems, the question is whether or not there is a possibility to create a phase mixture in a heavy ion collision. This question is twofold, because it depends on the timescale or speed of the dynamics of the process, as well as on the breakup density of the system.

The time scale of the development of larger size density fluctuations of 2-3fm is approximately 20-30fm/c as we estimated above. This is comparable with the typical expansion time of an average heavy ion collision. Thus if we have a large colliding system such as central Nb+Nb or U+U collisions, at the relatively low energies (around 100 MeV per nucleon) the expansion time is more than sufficient to form coexisting phases. In smaller systems the time might not be sufficient to develop a phase mixture, so supercooling may occur, or the system might even go through the unstable region being in one single phase all the time.

The other question is breakup. As we can see in Fig.1.2 a phase mixture can exist only below a certain density $n_L^{eq}(T)$ or $n_G^{eq}(T)$ which decrease with increasing entropy. At low total entropy (i.e. at low beam energies) the phase mixture may exist at densities slightly below n_0 while at higher entropies $\sigma_{tot} = 4$ the density should be below $n_0/40$. This is already very small compared to the lowest estimates of the breakup density $n_{BU} = 0.1\text{-}0.3 n_0$ [GG84b]. Consequently the system freezes out in high energy collisions where the average entropy $\sigma_{tot} > 4$, before phase mixture might be formed. In the few 100 MeV per nucleon energy region and below the formation of a phase mixture may preceed the breakup. This is just the energy region of the entropy puzzle.

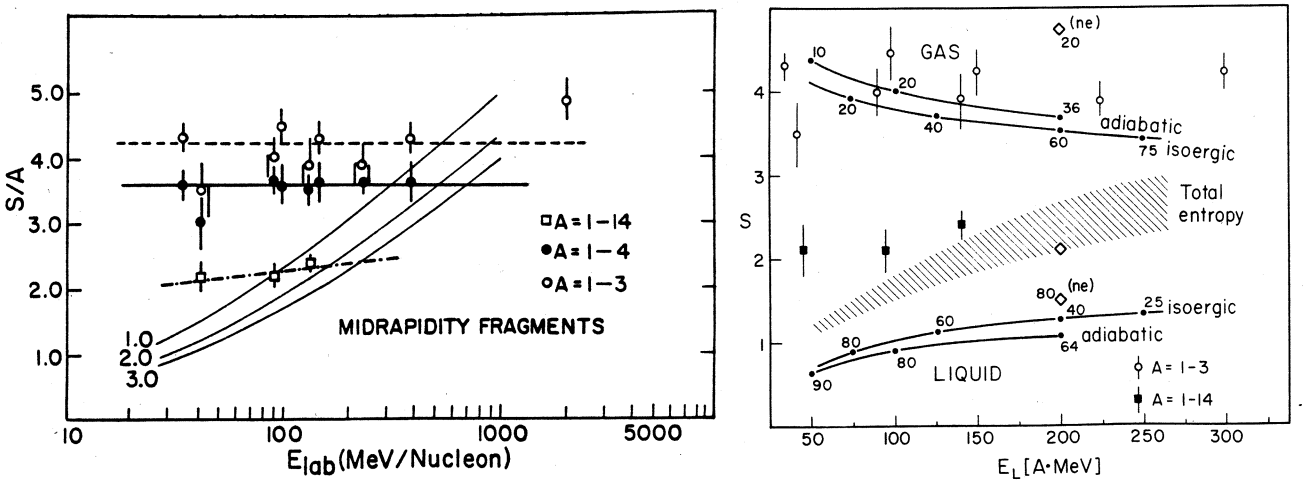

Fig. 2.2 (a) shows experimental results which seem to indicate that the entropy of the final state is not unique. From [JS84]. (b) This can be one indication of the liquid gas phase coexistence [Cs85] but, since the same result can be achieved by geometrical effects in noncentral collisions, this is not a conclusive evidence. Selection of central events would be desirable.

According to the arguments above it is reasonable to assume that a phase mixture develops in the final expansion stage of a reaction when the beam energy is not too high. This phase mixture may be in equilibrium or it may not. Nevertheless, the basic features of the phase mixture, such as $\sigma_L \ll \sigma_G$ and $n_G \ll n_L \approx n_0$, indicate that the

entropy may be essentially different for the two coexisting phases in a liquid-gas phase transition.

The delay of the phase transition was considered in ref. [Cs85]. It was assumed that the equilibration time for the pressure and temperature balance between the phases is short, but the chemical equilibration time τ_{ch} was assumed to be comparable with the timescale of the dynamics, $\tau_{ch} \propto u_T^2$. The first two of Gibb's criteria, $p_L=p_G$, $T_L=T_G$ were assumed to be satisfied. Thus the abundances of the liquid and gas phases should be evaluated by using the explicit equation (2.14). Following the phase transition dynamically resulted in a continuous increase of entropy according to eq. (2.13). The entropy increase obtained this way was $\Delta\sigma \approx 0.4$-0.5 (Fig. 2.3).

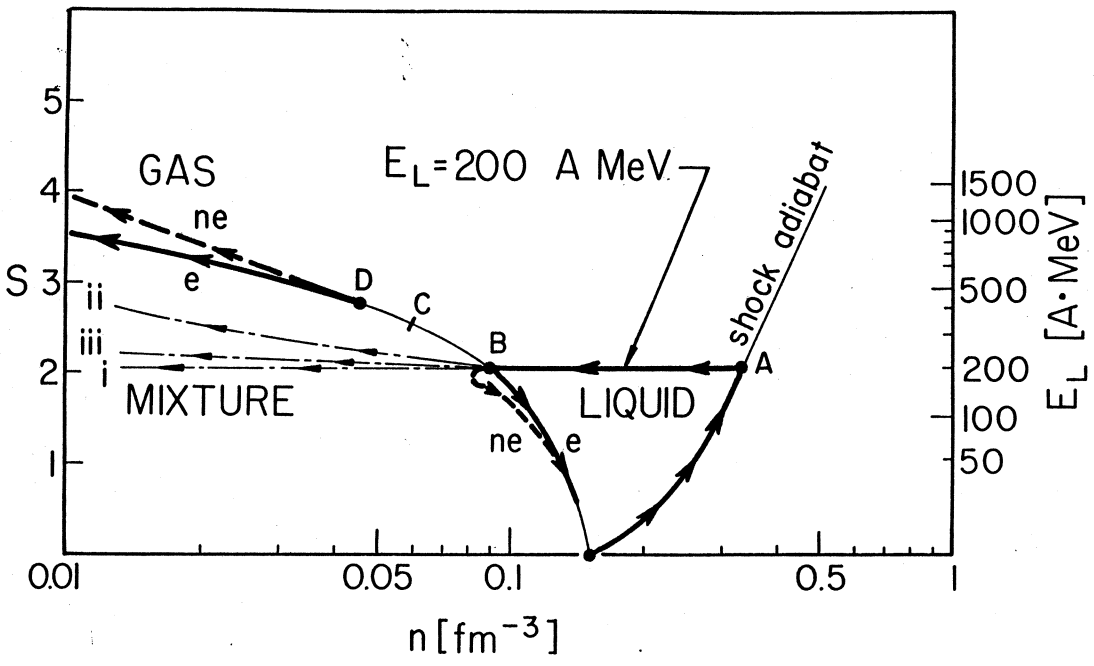

Fig. 2.3 Dynamical paths across the liquid gas phase transition region calculated in a fluid dynamical model (i) adiabatic expansion, (ii) isoergic exp., (iii) nonequilibrium expansion. From [Cs85].

This dynamical assumption resulted in a supercooled liquid phase in coexistence with a gas phase. Due to the parametrization $\tau_{ch} \sim u_T^2$ the liquid phase, however, never entered the unstable region.

In the nonequilibrium expansion scenario [Cs85] one of the Gibbs criteria requiring the equality of the chemical potentials of the two phases, was relaxed and replaced by an explicit rate equation for the creation of the newly formed phase (2.14). The rate of the phase growth was characterized by the relaxation time $T_{ck} = qu_T^2$. Apart from the extra entropy production, this delayed phase transition resulted in some interesting effects: The cooling was slowed down compared to the phase equilibrium by a factor of two (for q=10 fm/c), and the gas phase had a much smaller abundance (20-30%) at the breakup [CK86]. The extra entropy produced appeared in the larger entropy of the gas phase $\sigma_G > \sigma_G^{eq}$.

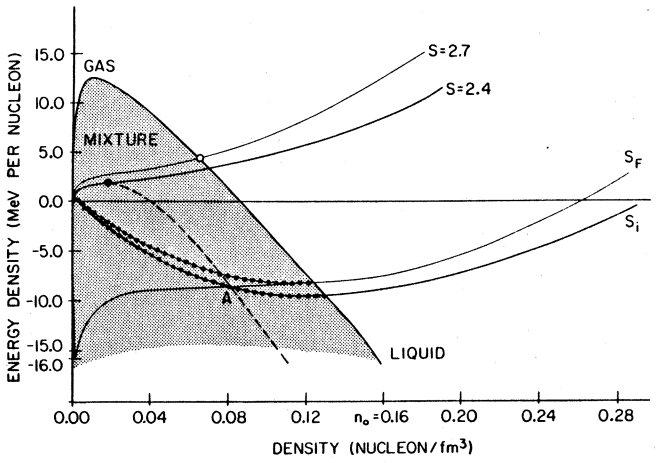

Fig. 2.4 Adiabatic expansion paths on the phase diagram. The curves which bend up at low and decreasing densities represent single phase expansions. If a system is supercooled in a single phase and reaches point A it is assumed to undergo a rapid phase equilibration and continue the expansion on an adiabat representing the mixed phase, which bends downwards. The entropy jumps at A. From [LS84].

Supercooling in the single liquid phase in adiabatic expansion was studied by Lopez and Siemens [LS84]. In Fig. 2.4 this can be viewed as

the system moving on a constant entropy line towards smaller densities, and entering the supercooled metastable region in the liquid phase. The adiabatic expansion was assumed to be continued in a single phase even when the system entered the unstable region. That is, in Fig. 2.4 we cross the thin full line corresponding to $u_T^2 = 0$.

The system forms a phase mixture and equilibrates rapidly when u_0^2 becomes zero at the dashed line in this scenario. This rapid equilibration happens at constant density n and energy density e, thus giving rise to a considerable entropy jump of $\Delta\sigma \approx 0.2\text{-}0.6$.

The entropy increase versus the initial entropy obtained in this scenario is plotted in Fig. 2.5. The maximum extra entropy, $\Delta\sigma \approx 0.6$, is produced when the initial entropy of the expanding system is $\sigma_{in} = 0$. This is due to the fact that in the adiabatic expansion through the metastable region the pressure is negative, so we have to invest energy - pdV to expand the system. This energy thermalizes and gives rise to a large entropy increase when the two phases equilibrate and the pressure becomes positive.

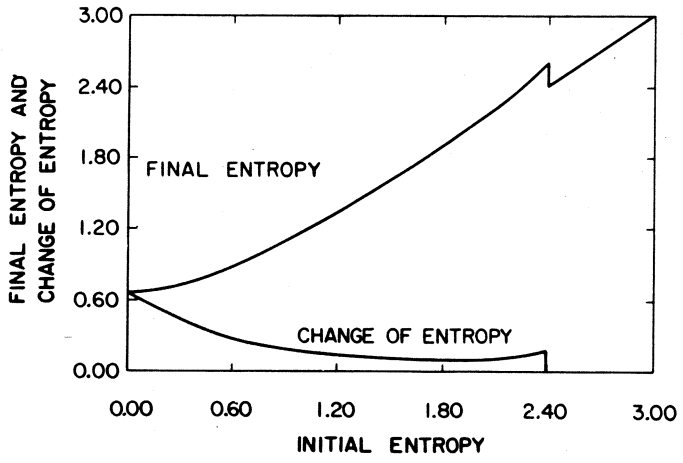

Fig 2.5 Final entropy and extra entropy produced in the expansion through the phase transition. Fron [LS84].

2.3 Dynamics of Equilibrium Phase Transition

At the end of an adiabatic or near adiabatic expansion the system may reach the boundary of the phase equilibrium n_L^{eq} or n_G^{eq}. In order to study the dynamics of the phase transition the equation of state of the phase mixture should be coupled to the equations of fluid dynamics determining the time evolution of the expansion. The fluid dynamical equations provide us with the local density n(t) and entropy density s(t) if the equation of state p=p(n,s) or p=p(ν,σ) is given.

In the equilibrium phase mixture, where Gibb's criteria are satisfied the equilibrium values of the extensives n, s, e,.... or ν σ, ϵ,..... depend on only one intensive which may be the temperature T but could also be the pressure p or the chemical potential μ. Then the equation of state of the phase mixture p=p(ν,σ) necessary to solve the fluid dynamical equations can be obtained as the solution of the following system of equations.

$$\nu = \alpha_G \nu_G^{eq}(p) + \alpha_L \nu_L^{eq}(p) \tag{2.16}$$

$$\sigma = \alpha_G \sigma_G^{eq}(p) + \alpha_L \sigma_L^{eq}(p) \tag{2.17}$$

where $\alpha_L+\alpha_G=1$. Note that $\nu_G^{eq}(p)$, $\nu_L^{eq}(p)$, $\sigma_G^{eq}(p)$, and $\sigma_L^{eq}(p)$ are known. Thus not only p(t) but also the unknowns $\alpha_G(t)$ and $\alpha_L(t)$ can be determined, and so eliminated analytically from eqs. (2.16-17). Then the equation of state p(ν,σ) is given as the solution of the following equation:

$$[\sigma-\sigma_L^{eq}(T)](\nu_G^{eq}(P)-\nu_L^{eq}(p)] = [\nu-\nu_L^{eq}(p)][\sigma_G^{eq}(p)-\sigma_L^{eq}(p)] \tag{2.18}$$

Having obtained p, the phase abundances at a given t, when the specific volume is $\nu=\nu(t)$, are given by

$$\alpha_G = \frac{\nu - \nu_L^{eq}}{\nu_G^{eq}(p) - \nu_L^{eq}(p)} \qquad (2.19)$$

These equations were solved in [SK84,Cs85,GC86]. In [SK84] the time dependence of the density n was studied assuming adiabatic flow. At low initial entropy, σ=1 and density $n=n_0$, a very long expansion time of 80fm/c was obtained assuming phase equilibrium. When the formation of phase mixture was forbidden the calculation showed an oscillating density solution, like the monopole giant resonance, due to the fact that the matter entered the unstable, negative pressure region of the phase diagram.

When the formation of phase mixture was allowed a small amount of gas phase was formed until the breakup at $n_{BU}=n_0/3$ was reached. The abundance of this gas phase was found to be α_G=3% (20%) for an initial entropy of σ = 1(2). Formation of a phase mixture at higher entropies was not considered there.

In [Cs85,CG86] equilibrium dynamical phase transitions were considered. In a near adiabatic expansion even above the critical entropy σ_c= 2.5 a phase separation is possible because the system cools down in the expansion. Thus not only bubbles but droplets of the fluid phase can also be formed. The temperature during the expansion is decreasing and only the breakup temperature can be measured. Thus both high entropy and low entropy expansions should be considered. The simplified fluid dynamical equations were solved by the EOS given in eq. (2.18). The dynamical phase transition assuming chemical equilibrium $\mu_G=\mu_L$ was faster than the nonequilibrium one and somewhat more gas phase is produced during the expansion.

Although the phase equilibrium is maintained in these calculations and so entropy increase due to chemical nonequilibrium was not possible, dissipation and entropy increase, due to other reasons like viscosity are possible. The most dissipative collision possible is the one where

the internal energy of the particles is constant i.e. the speed of expansion is constant. In this case eq. (2.17) should be replaced by

$$\varepsilon = \text{const} = \alpha_G \varepsilon_G^{eq}(p) + \alpha_L \varepsilon_L^{eq}(p), \tag{2.20}$$

which will lead to straightforward changes in eqs. (2.18-19). Fig. 2.6.

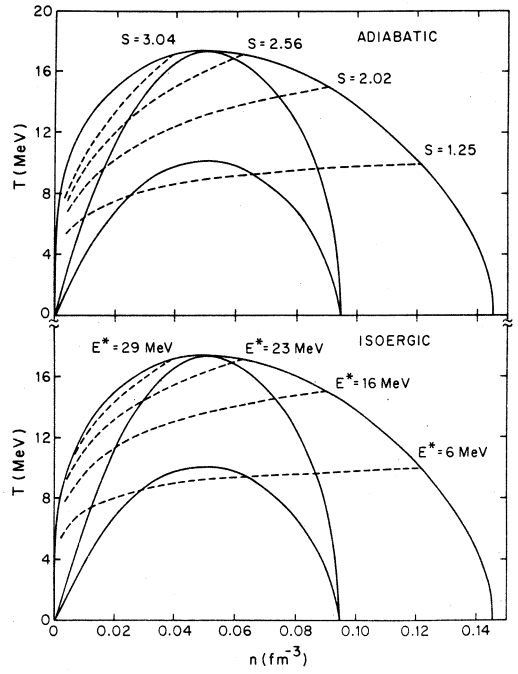

Fig. 2.6 Adiabatic and Isentropic pathes through the phase transition in complete phase equilibrium (dashed lines). From [GC86].

If we are not interested in the explicit time dependence of the expansion in phase equilibrium, the description of the two limiting cases is very simple [CG86]. In an adiabatic expansion eq. (2.17), in an isoergic expansion expansion eq. (2.20) is satisfied with the constant entropy or energy. Then (2.16) gives the relation directly between the density and pressure (temperature) during the expansion while (2.19) gives the phase abundances in an explicit form. The only information necessary is the behavior of the equation of state along the Maxwell construction line $n_G^{eq}(T)$, $n_L^{eq}(T)$, $o_G^{eq}(T)$, $o_L^{eq}(T)$, and $\varepsilon_G^{eq}(T)$, $\varepsilon_L^{eq}(T)$. The most striking difference between the adiabatic and isoergic expansion appears in the behavior of fragment abundances α_G and α_L

[CG86], which are larger and increasing essentially faster in the isoergic expansion with decreasing temperature.

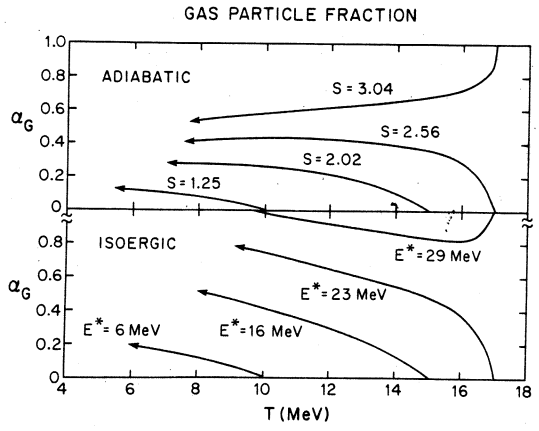

Fig. 2.7 The fraction of barion number carried by the gas phase for trajectories shown in Fig. 2.6. From [GC86].

2.4 Droplet formation rate

To perform a realistic calculation of a dynamical phase transition one needs quantitative information about the transition rates. This information is implicitly available in molecular dynamics models [VJ85,AS86] and to some extent in transport models (VUU-BUU-BN) [BB86b,DG86b]. So far in none of these studies the droplet formation or evaporation rates were evalauted systematically but the possibility of forming two phases was demonstrated [VJ85].

The droplet formation rate was explicitly evaluated [Gr86] along the Maxwell construction line in a rate equation approach recently. In a container of given pressure and temperature the probability or yield of forming a droplet of mass A in a gas depends on the change of the Gibbs free energy:

$$Y(A) \propto \exp[-\Delta G(A)/T]. \qquad (2.21)$$

Given that $\Delta G = G_{\text{with drop}} - G_{\text{no drop}}$, where

$$G_{\text{no drop}} = \mu_G(A+B) \qquad (2.22)$$

$$G_{\text{with drop}} = \mu_G B + \mu_L A + 4\pi R_A^2 \sigma + T\tau \ell n A, \tag{2.23}$$

the yield of A-particle droplets can be written as:

$$Y(A) \propto A^{-\tau} \exp\left[\left(\frac{\mu_G - \mu_L}{T}\right) A - \frac{4\pi r^2 \sigma}{T} A^{2/3}\right] . \tag{2.24}$$

Here $R_A = rA^{1/3}$ is the radius of the droplet, and $(n_L)^{-1} = \frac{4}{3}\pi r^3$ is the density of the liquid phase. The $\sigma(T)$ is the surface tension, and τ is Fisher's constant. See more in sect. 3. Along the phase boundary $\mu_G = \mu_L$. Adjusting the exponential to insure continuity at A=1, one can write an expression for the equilibrium concentration for droplets of size A:

$$Y^{EQ}(A) = Y^{EQ}(1)\, A^{-\tau} \exp\left[\frac{-4\pi r^2 \sigma}{T} (A-1)^{2/3}\right] \tag{2.25}$$

This equation gives the distribution Y^{EQ} that a metastable vapor phase should converge towards, given sufficient reaction time.

The time rate of change of A-particle droplet concentrations can simply be approximated by

$$\frac{dY(A)}{dt} = G_A - L_A . \tag{2.26}$$

Here G_A defines the rate of gain of A-particle droplets, and L_A the rate of loss of A-particle droplets.In [Gr86] it was assumed that droplets may grow or shrink only by reactions which involve the addition to or the subtraction of single nucleons. Given this assumption there are four possible processes by which an A-size droplet can be gained:

$$G_A = D_{A+1,1} Y(A+1) + C_{A-1,1} Y(A-1)Y(1) + B_{A+1,1} Y(A+1)Y(1) + F_{A-1,1,1} Y^2(1)Y(A-1). \tag{2.27}$$

Likewise similar arguments can be used to obtain an expression for the loss term:

$$L_A = D_{A,1}Y(A)+C_{A,1}Y(A)Y(1)+B_{A,1}Y(A)Y(1)+F_{A,1,1}Y^2(1)Y(A) \qquad (2.28)$$

The rate coefficients C, D, B, and F are not independent, however. Consider three physical relationships which can be used to define them: detailed balance, collision cross sections, and particle conservation.

The principle of detailed balance requires that a steady state must exist at equilibrium: $\dot{Y}(A) = 0$ or $G_A^{EQ} = L_A^{EQ}$. For illustration consider the following reaction process:

$$1 + (A-1) \overset{EQ}{\rightleftarrows} A$$

or

$$C_{A-1,1}Y^{EQ}(A-1)Y^{EQ}(1) = D_{A,1}Y^{EQ}(A). \qquad (2.29)$$

Eq. (2.29) imposes constraints on C and D, and equations resulting from the three other reaction processes likewise constrain F and B.

The second limitation on the rate coefficients is that of the collision cross section. Consider a typical breakup reaction 1+A → 1+1+(A-1) where a fast gas particle collides with an A-size droplet breaking off a piece. The breakup coefficient $B_{A,1}$ was calculated [Gr86] from a thermal-averaged breakup cross section $\sigma_{A,1\ B\text{-}up}$ where $B_{A,1} = \langle \sigma_{A,1\ B\text{-}up} \cdot v \rangle$ and

$$\sigma_{A,1\ B\text{-}up} = \pi R_A^2 \left(1 - e^{-mv^2/2T}\right) \quad . \qquad (2.30)$$

Equation (2.30) is used as the relevant parametrization for $\sigma_{A,1\ B\text{-}up}$ since it illustrates the expected dependence of the cross

section on a geometric term πR_A^2, and on an energy-dependent term ($1-e^{-mv^2/2T}$) which increases the likelihood of breakup as the relative velocity increases. If the particles are given a Maxwell-Boltzmann energy distribution one obtains an expression for $B_{A,1}$:

$$B_{A,1} = 4\pi \left(\frac{m}{2\pi T}\right)^{3/2} \int v^3 \, e^{-mv^2/2T} \sigma(v) dv$$

which can be integrated to give

$$B_{A,1} = 3 \left(\frac{\pi T}{2m}\right)^{1/2} R_A^2 \, . \tag{2.31}$$

Likewise the thermal averaged condensation cross section, $\sigma_{A,1 \text{ condensation}}$, can be equated with the condensation rate coefficient for a reaction $1+A \rightarrow (A+1)$ where a low-energy gas particle collides and fuses with an A-size droplet:

$$C_{A,1} = \left(\frac{\pi T}{2m}\right)^{1/2} R_A^2 \, . \tag{2.32}$$

The two other rate coefficients can now be related back to $C_{A,1}$ and $B_{A,1}$ through detailed balancing.

The third constraint on C, B, D, and F is that of particle conservation. This requires that the baryon density must remain constant--no particles may be added or taken away at any step in the evolution of the system.

$$\sum_{A=1}^{N} A\dot{Y}(A) = 0 \tag{2.33}$$

Here N is the total number of gas particles in the system initially. This constant essentially restricts the incremental expansion or reduction of the rate coefficients as the droplet size is increased or

decreased, yielding expressions for the rate coefficients for droplets of size other than A.

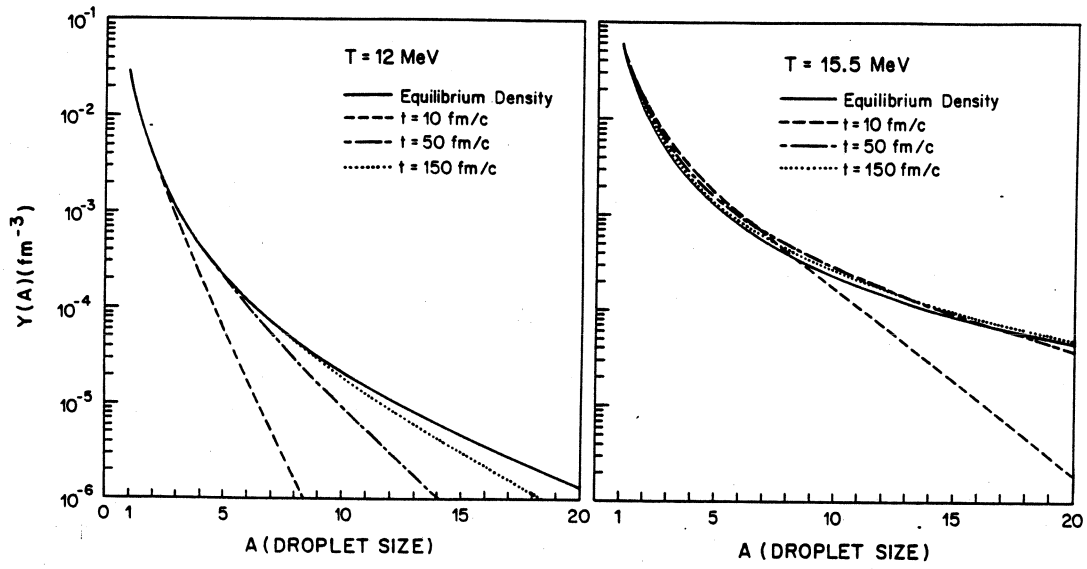

Fig. 2.8 Droplet size distributions at different times calculated in a rate equation model. From [Gr86].

Finally a full rate equation can be written for the change of A-particle droplet concentrations in time.

$$\dot{Y}_{(A)} = \left(\frac{\pi T}{2m}\right)^{1/2} r^2 \left[Y^{EQ}(1)\{\exp[X[X(A-1)^{2/3} - A^{2/3}]][A^{2/3-\tau}(A+1)^{\tau}Y(A+1)\right.$$

$$\left. - \exp[X[(A-2)^{2/3} - (A-1)^{2/3}]](A-1)^{5/3-\tau}A^{\tau-1}Y(A)]\right\}$$

$$+ 3\,Y^2(1)/Y^{EQ}(1)\{\exp[X[(A-1)^{2/3} - (A-2)^{2/3}]]A^{2/3-\tau}(A-1)^{\tau}Y(A-1)$$

$$\left. - \exp[X[A^{2/3} - (A-1)^{2/3}]](A+1)^{5/3-\tau}A^{\tau-1}Y(A)\right\} - 4Y(A)Y(1)A^{2/3}$$

$$+ Y(1)/A\{(A-1)^{5/3}Y(A-1) + 3(A+1)^{5/3}Y(A+1)\}] \qquad (2.34)$$

Here $X = \frac{-4\pi r^2 \sigma}{T}$. For N gas particles there will exist N such equations, each coupled to the others through their dependence on droplet concentrations of one size larger and one size smaller. This system of equations was solved numerically [Gr86]. A steady convergence to equilibrium was found. Typically, reaction rates increase with temperature, so that the approach to equilibrium is more rapid at higher temperatures. Fig. 2.8.

Relevant times for heavy-ion reactions are on the order of 50 fm/c, and at this time, deviation from equilibrium was observed [Gr86] especially for heavier fragments. The assumptions in this calculation were on the conservative side: $\mu_L = \mu_G$ and only single nucleon exchange were assumed. Even the relaxation times were found to be ≈10, 50, 150 fm/c at temperatures T=15.5, 12, 8 MeV respectively for a fragment of mass A=7.

3. Finite Systems and Fragment Abundances

3.1 Phase transition in finite systems

For a system with a finite number of particles in a very strict sense no phase transitions exist and fluctuations can be important. Could it be that nuclear systems are so small that these fluctuations completely wash out the first order liquid-gas phase transition below T_c? This question was first addressed in the context of heavy ion reactions in [GK84]. Consider a system held at fixed temperature and pressure. We are interested in density fluctuations of this system. Instead of a nuclear system it may be helpful to think of a finite number of particles placed in a cylinder which is maintained at a fixed temperature T, with a movable piston at one end which exerts a constant pressure p on the gas particles. Only a finite number of particles per unit time collide with the piston, so the position of the piston will fluctuate with time about some mean position. Thus the density of the gas will also fluctuate.

The ratio of probabilities for a system to be at density n_1 or n_2 is

$$P(n_2)/P(n_1) = \exp\left[-(G(n_2) - G(n_1))/T\right] \qquad (3.1)$$

where G(n) is the Gibbs free energy at p and T. For an infinite system in equilibrium the density n is determined by the equation of state once p and T are specified. It is necessary therefore to know G(n) for densities not permitted by the equation of state. This is provided by the Landau theory [LL54] in which n is treated as an independent variable not restricted by p and T. Such an analysis was carried out in [GK84]. A simple form for the nuclear EOS was chosen

$$p = -a_0 n^2 + 2a_3 n^3 + nT \qquad (3.2)$$

(a_0=293 MeV fm^3, a_3=666 MeV fm^6, n_0=0.15 fm^{-3}, B=8 MeV) which has a critical point at $n_c=a_0/(6a_3)$, $T_c=a_0 n_c$, $p_c=\frac{1}{3} T_c n_c$. One can expand the EOS (3.2) around the critical point by introducing $t=T-T_c$ and $\eta=n-n_c$,

$$p-p_c = n_c t + t\eta + 2a_3\eta^3. \tag{3.3}$$

This equation of state behaves similarly to the Van der Waals EOS, for negative t the phase equilibrium points can be found by the Maxwell construction [GK84]:

$$\eta_L = -\eta_G = \sqrt{-t/2a_3} \tag{3.4}$$

The essential feature of the Landau approach is the construction of the free energy in terms of a power series in the order parameter η. Thus $G(p,T,\eta)$ will be defined at nonequilibrium values of η too, for a fixed p and T. In the neighborhood of the critical point the Gibbs free energy is then:

$$G(p,T,\eta) = G_c(p,T,\eta) + \alpha(p,T)\eta + A(p,T)\eta^2 + C(p,T)\eta^3 + B(p,t)\eta^4 + \ldots \tag{3.5}$$

The EOS (3.3) can be used to obtain the coefficients in (3.5) since the equilibrium value of η can be obtained from the requirement that G has an extremum in equilibrium:

$$\frac{\partial G}{\partial \eta} = \alpha + 2A\eta + 3C\eta^2 + 4B\eta^3 = 0 \tag{3.6}$$

This should be the EOS (3.3). Comparing (3.3) and (3.6) we obtain for the coefficients:

$$\alpha = -(p - p_c - n_c t)D \ ,$$

$$A = \frac{1}{2} \cdot tD \ ,$$

(3.7)

$$B = \frac{a_3}{2} D ,$$

$$C = 0 ,$$

where $D = N/n_c^2$ and N is the number of nucleons. This choice of D gives the correct G for equilibrium states. So the G in the order parameter expansion is

$$G = G_c(p,T) + \frac{N}{n_c^2} \left[-(p - p_c - n_c t)\eta + \frac{1}{2} t\eta^2 + \frac{a_3}{2} \eta^4\right] \qquad (3.8)$$

The density or η values at the phase equilibrium η_L and η_G are the solutions of the EOS (3.3) if $p=p_c+n_c t$. The probability that at this pressure $p=p_c+n_c t$ the density distribution of the system is given by

$$R(n) = \frac{P(n)}{P(n_L)} = \exp\left[-(G(p,T,\eta) - G(p,T,\eta_L))/T\right] \quad . \qquad (3.9)$$

This probability is plotted in Fig. 3.1

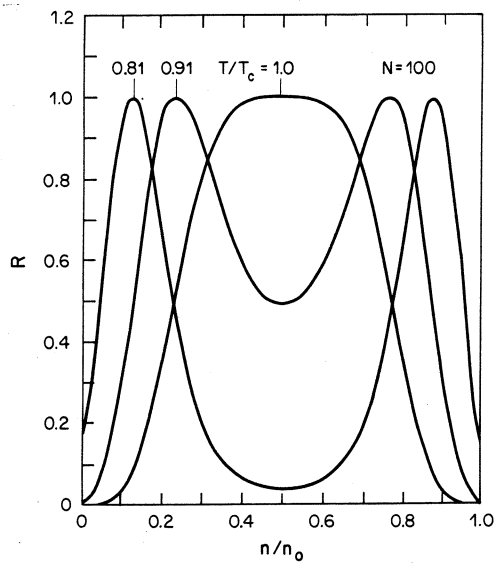

Fig 3.1 R is the relative probability for the system to be at density n compared to the thermadynamically favored values n_G or n_L . The number of nucleons is 100. The pressure is the equilibrium oressure. From [GK84].

It shows the relative probability R for the system of 100 nucleons to be at density n compared to the thermodynamically favored densities of n_L (liquid density) and n_G (gas density). For T not too close to T_c there are two well defined peaks corresponding to a separation of liquid and gas phases, thus exhibiting a reasonably sharp first order phase transition. As T approaches T_c from below the valley separating the two peaks gets filled in and the distinction between liquid and gas gets washed out. At T_c the distribution is flat at the top. These large density fluctuations at the critical point give rise to the phenomenon of critical opalescence in atomic systems.

To find the relative probability for a system composed of N nucleons, N not necessarily 100, one simply scales the results of Fig. 3.1 to the power N/100, $R^{N/100}$, because in eq. (3.9) the Gibbs free energy was taken to be proportional to the total number of particles. For the density midway between n_L and n_G the relative probability assumes the simple form

$$R\left(\frac{n_L+n_G}{2}\right) = \exp\left\{-\frac{3}{4}(T - T_c)^2 N/(TT_c)\right\} \qquad (3.10)$$

Thus a larger number of nucleons N sharpens the distinction between liquid and gas phases.

For a finite nuclear system statistical fluctuations are important not only at the critical point, but in some neighborhood of the critical point. These fluctuations provide a mechanism for the system to enter the metastable and unstable regions of the phase diagram. For 100 nucleons and $0.9<T/T_c<1$ the fluctuations are large and it is improper to speak of a sharp first-order phase transition. As the temperature is lowered the fluctuations diminish in amplitude and the first-order phase transition gradually emerges.

3.2 Fragment mass distribution

There are numerous models describing fragment mass distributions. A concise review is given in ref. [CK86]. The overwhelming majority of the models describe a static situation at the "freeze-out moment". It is possible that at this moment some excited nuclear fragments exist and their final decay by particle emission is also considered in the most sophisticated calculations [SB83,FR83,BB86,CK86b]. Most models are of statistical origin and in principle they would yield an equation of state. (This is not so in some percolation models where the connection between the bond-breaking probability and physical quantities like energy and density is not defined.) The evaluation of the equation of state is, however, not a trivial task and in practice it is very seldom performed [CF86b]. Thus it is not always clear whether a statistical model which satisfactorily describes the experimental data exhibits a liquid-gas phase transition or not. Here only some very basic facts will be mentioned about the fragment distributions and a few of the recent works not mentioend in [CK86] will be discussed.

We have seen that both in equilibrium and in nonequilibrium expansion if finally two phases exist, they are very different. The gas phase is very dilute and has a large entropy $\sigma_G \approx 3.5\text{-}4$, while the liquid phase has low entropy $\sigma_L \approx 1\text{-}2$ and density close to n_0. What is the fragment distribution in such a phase mixture? The gas phase, having large entropy, consists of very light fragments with an exponentially decreasing mass spectrum. In this limit there is not much difference in the model estimates. From the experimentally observed light fragment (proton to alpha) abundances all previously discussed models extract an entropy value on the order of 3-4, down to a few 100 MeV beam energy or even lower [Ka84, JS84].

The prediction of the mass distribution of heavier fragments representing the liquid phase is a more involved problem. The thermodynamical limit does not yield a definite prediction. Surface effects, nuclear size, reaction geometry, fission, final state decays and even the collective flow pattern may influence the intermediate and heavy fragment mass distribution. The light fragment distributions are not independent of the liquid phase. The final decay or fission of the

heavier fragments can change the light fragment distributions too. While for the light fragments the grand canonical treatment is acceptable, the behavior of intermediate mass fragments is already strongly influenced by the limited nucleon number.

3.3 Law of Mass Action

The law of mass action as applied to ideal gases is the most basic law describing the fragment distributions. Ignoring relativistic, quantum and isospin effects (these are easily put back in) the number density of ground state nuclei of mass number A is

$$n_{gs}(A) = g_A(\frac{mTA}{2\pi})^{3/2}\ e^{A(\mu+B)/T} \tag{3.11}$$

where g_A is the spin degeneracy, m is the nucleon mass and B>0 is the binding energy per nucleon. The nonrelativistic chemical potential per nucleon μ is related to the relativistic chemical potential by $\mu = \mu_{rel} - m$. If $\mu < -B$ then the number density is a decreasing function of A. Once $\mu = -B$ the nuclei would like to coalesce, to form uniform liquid nuclear matter. Another way to see this is to put the quantum statistics back. Then the point at which $\mu=-B$ is where Bose-Einstein condensation of the bosonic nuclei would occur.

Using eq.(3.11) for p and d: $x = n_d/n_p = 3/2\ 2^{3/2}\ e^{\mu/T}$, it follows that $\mu/T = \ln x - 1.445$. Now from $\varepsilon = T\sigma - \nu p + \mu$ by inserting the Boltzmann ideal gas expressions $\varepsilon = 3T/2$ and $p = nT$ we get $\sigma = -\mu/T + 2.5$. Using the expression of μ/T in terms of x we can express the entropy by the d/p ratio: $\sigma = 3.945 - \ln x$ [SK79].

Not only nuclei in their ground states but also nuclei in various excited states will be present. To explicitly count them we should additively include

$$n(A)_{i*} = \frac{g_i}{g_A} \cdot n(A)_{gs} \cdot e^{-E_{i*}/T} \tag{3.12}$$

where g_i is the degeneracy of the excited state and E_{i*} is its excitation energy above the ground state. If the total baryon density is known as usual, μ can be obtained from

$$n = \sum_A \sum_{i,gs} A\, n_i(A) \qquad (3.13)$$

Several groups have written computer codes to calculate the nuclear fragment mass distribution using the law of mass action for ideal gases. In [RK81, FR82, FR83, RF82] all known nuclear states with $A<16$ having a width $\Gamma<1$ MeV were included explicitly, and these levels for $A>4$ were supplemented by an effective level density formula for the higher lying states which are not known experimentally [FR83, FR86]. Since this model includes an excluded volume approximation, the equation of state belonging to this is different from the ideal gas equation of state, Fig. 3.2.

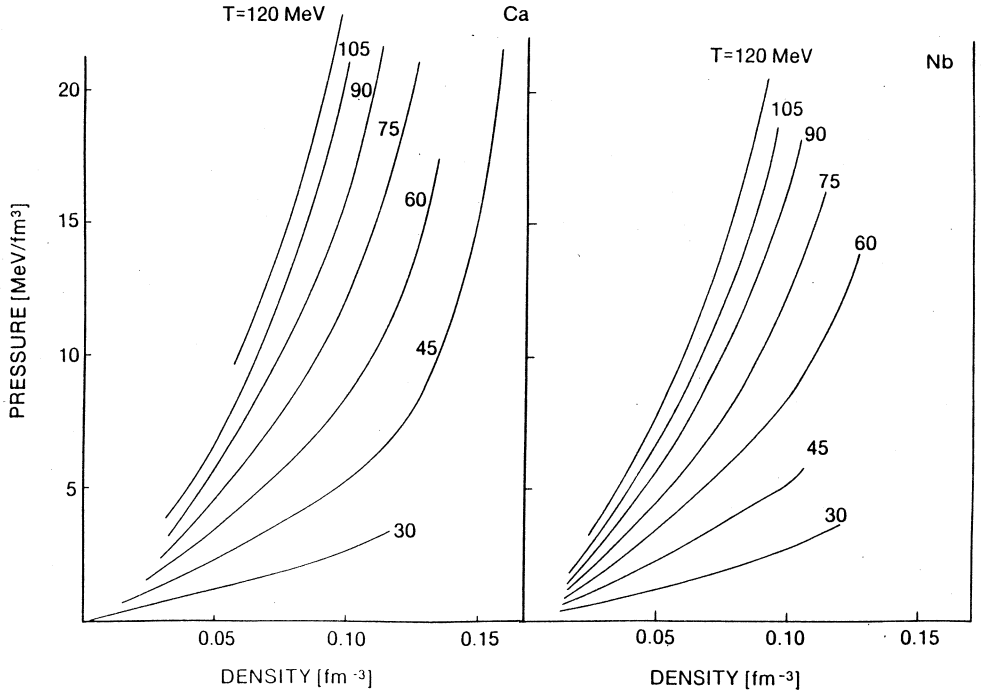

Fig. 3.2 Equation of state underlying the FREECSO calculations, with the excluded volume approximation. There is no phase transition due to the absence of attractive interactions. From [CF87].

It does not show a first order phase transition because only repulsive interactions are included, long-range attraction is not. This

code has recently been named FREESCO [FR86]. It is an approximate microcanonical event generator where the exact microcanonical fragment distribution is calculated recursively by approximating the one-fragment inclusive distributions in each step by the grand canonical distribution.

Another fragmentation model is the Quantum Statistical Model (QSM) [SC81,SB83] which calculates the grand canonical one-fragment inclusive

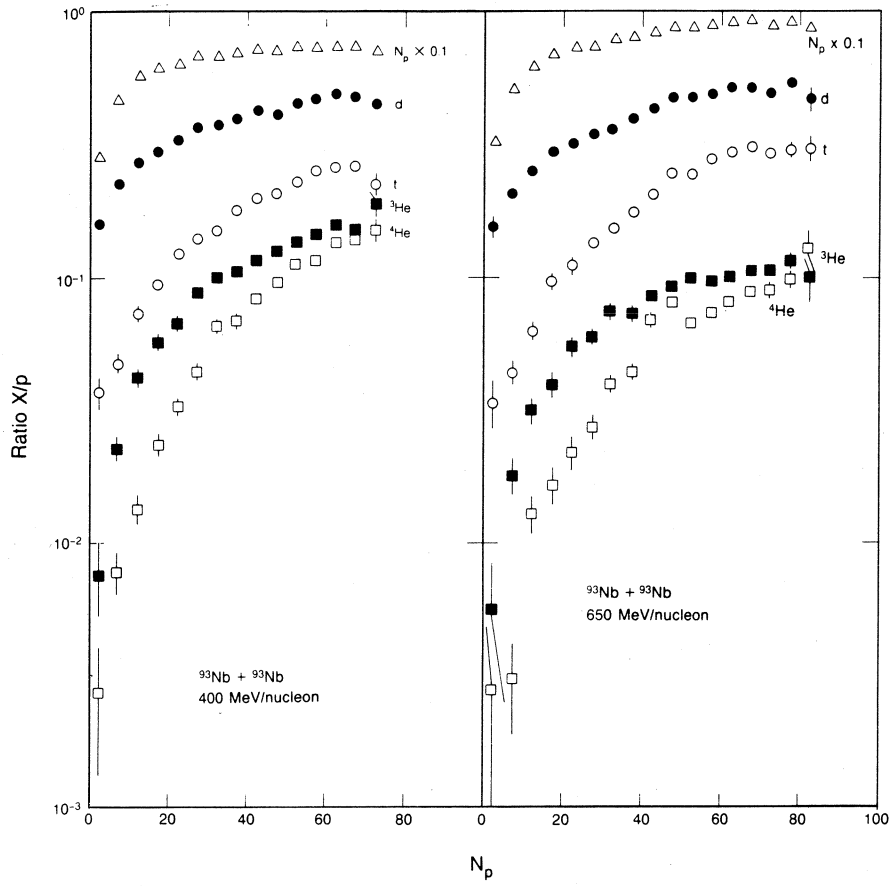

Fig. 3.3 Ratios of the produced composite particles X=(d,t,...α) to protons as a function of the proton multiplicity for two different systems. From [DG85].

distribution functions, but it includes as a special feature quantum statistics. The known particle-stable and metastable nuclear states with A<20 are included in this model, and the repulsive interactions are simulated by the excluded volume approximation.

Both models are based on the same physical picture: namely a first fast explosion creating light and medium mass fragment according to the law of mass action followed by sequential evaporation from these products in a final decay step.

These two models, which can be regarded as different implementations of a general statistical model for nuclear disassembly, were compared to each other and to experimental results recently [CK86b]. From the final fragment abundances the quantity

$$x = \frac{\text{d-like}}{\text{p-like}} = \frac{\text{d+1.5t+1.5 } ^3\text{He+3}\alpha}{\text{p+d+t+2 } ^3\text{He+2}\alpha} \qquad (3.14)$$

was calculated in both models for different breakup densities and temperatures. According to eqs. (3.2-3) these quantitites influence the

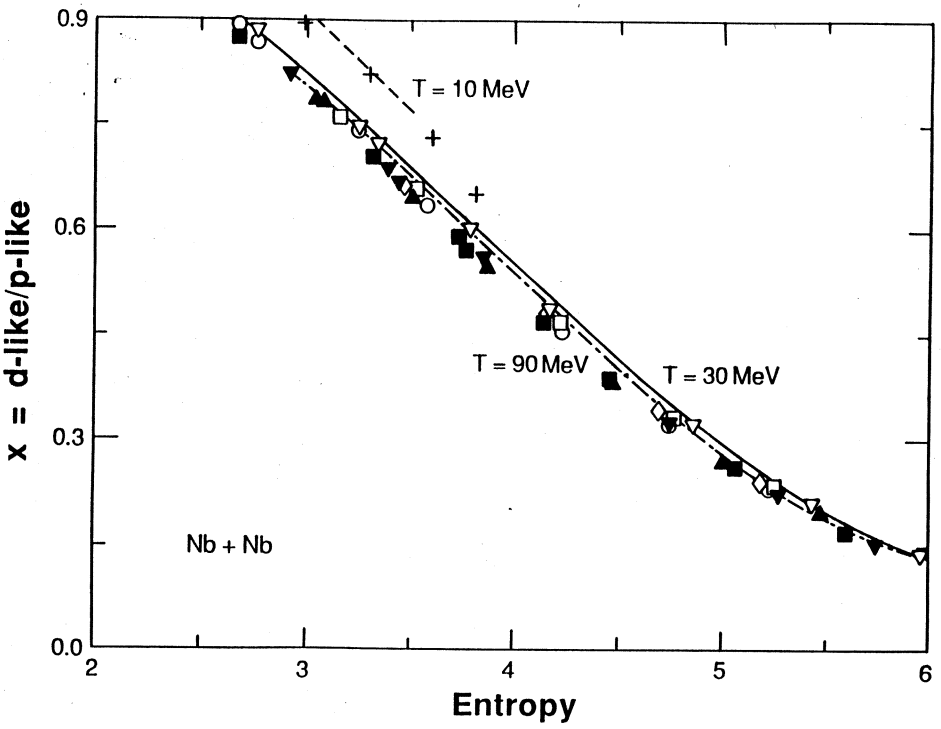

Fig. 3.4 d-like to p-like ratio calculated in the FREESCO (points) and QSM (curves) models. T=10,30,45,60,...120 MeV calculations correspond to +,∇,□,open diamomd, circle, filled up, down triangle, and square respectively. From [CK86b].

fragment distributions. It was found that in the breakup temperature range of T=30-90 MeV there is an essentially unique relationship between the quantity x and the entropy of the ideal gas mixture S. The lower temperature isotherms begin to deviate from the universal curve at low entropies, Fig. 3.4. At high entropies and low x the "Siemens-Kapusta" formula [SK79]

$$S = 3.945 - \ln x, \tag{3.15}$$

is a good approximation to the results of the more sophisticated statistical models. The experimentally determined values of x at the maximum charged particle multiplicity for different experiments ranging from 400 to 1050 MeV/nucleon beam energy [DG85] are between 0.48 and 0.68. According to Fig. 3.4 this yields entropy values of S=3.45-3.9 at the breakup.

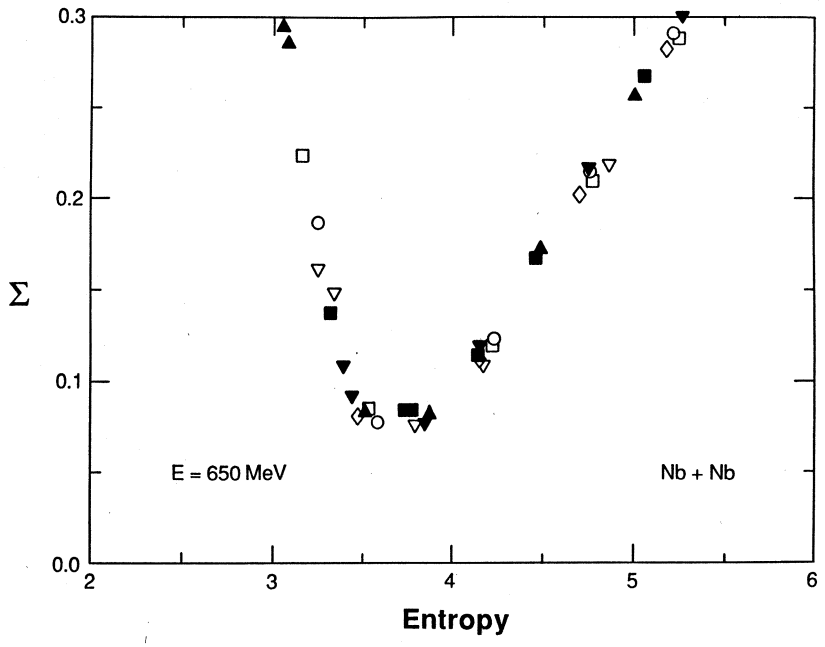

Fig. 3.5 Plot of Σ representing the deviation between theory and experiment [DG85], versus the entropy per nucleon for different temperatures. From [CK86b].

An alternative new method of comparing the theoretical results with experiment was introduced in [Ck86b] too. The function

$$\Sigma = \left[\left(\frac{d}{p}\right)_{theo} - \left(\frac{d}{p}\right)_{exp}\right]^2 + \frac{9}{4}\left[\left(\frac{t}{p}\right)_{theo} - \left(\frac{t}{p}\right)_{exp}\right]^2 + \frac{9}{4}\left[\left(\frac{^3He}{p}\right)_{theo} - \left(\frac{^3He}{p}\right)_{exp}\right]^2 + 4\left[\left(\frac{\alpha}{p}\right)_{theo} - \left(\frac{\alpha}{p}\right)_{exp}\right]^2, \tag{3.16}$$

should have its minimum at the best fit. Since the theoretical values depend on T and n this best fit also tells us the thermodynamical quantitites fitting the experiment the best. If this minimum is close or equal to zero, then the theory describes the fragmentation at the breakup correctly, and one can extract the thermodynamical parameters leading to this best fit. Furthermore the valley around the minimum of Σ with respect to a given thermodynamical parameter indicates the accuracy of the estimated parameter. As before this analysis also shows that the entropy per baryon can be uniquely determined this way from the experiment [DG85] while the breakup temperature and density remains

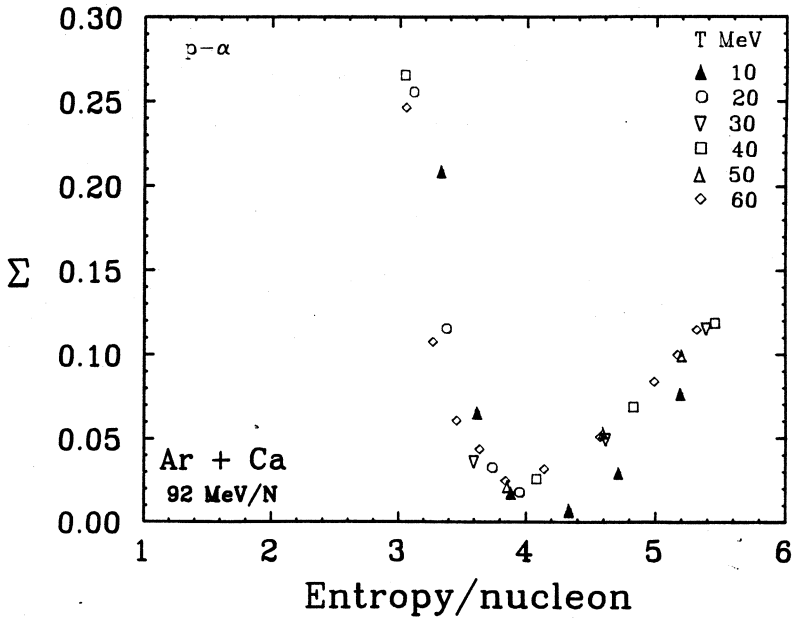

Fig. 3.6 Plot of Σ for Ar+Ca at 92 MeV/nucl. Experimental data are from [JW87]. From [CF87].

uncertain. Using additional experimental input (energy specta, two particle interferometry) one can estimate the breakup temperature being

T_{BU}=25-55 MeV and density of the order of $n_{BU}=\frac{1}{3} - \frac{1}{10}\, n_o$. The entropy on the other hand can be extracted more accurately and for the above reactions [DG85] it lies in the S=3.6-4.1 range which is consistent with the previous result [CK86b]. Fig. 3.5

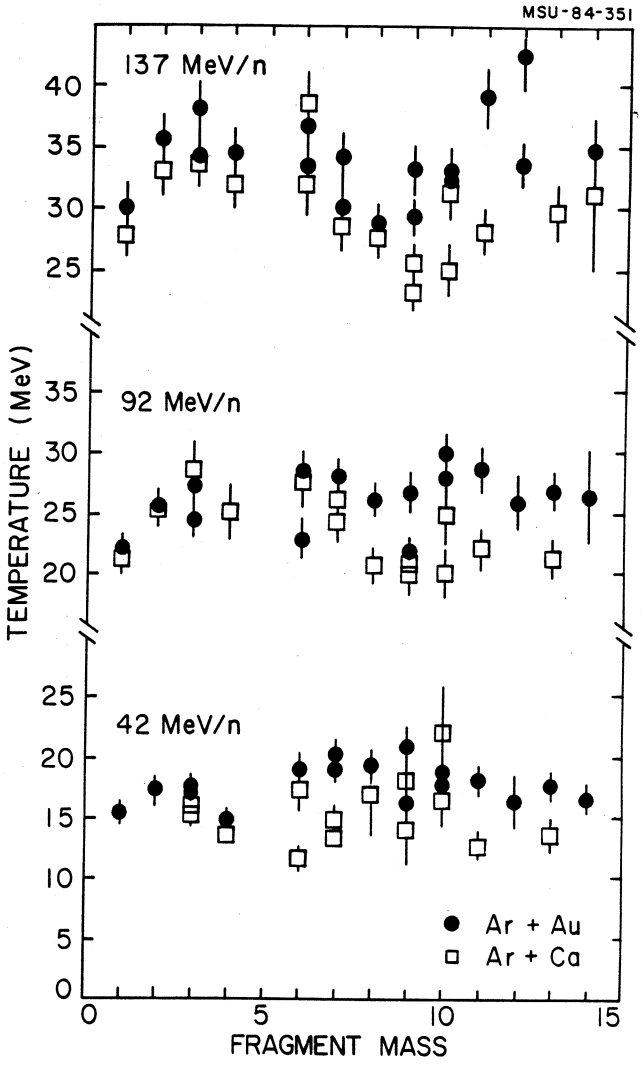

Fig. 3.7 Temperatures extracted from the energy spectra of different fragments with a moving source fit from intermediate energy heavy ion reactions. The temperatures are impressively constant independently of the particle! This might suggest thermal and phase equilibrium. From [JW87].

The above-mentioned experiments [DG85] are of relatively high energy and we do not expect the system to reach the nuclear liquid-gas phase transition before breakup. Therefore the above theoretical models which neglect attractive interactions yield satisfactory results. At lower energies the same is not true anymore [JW87]. While the apparent temperature of the spectra is the same for all fragments T=15-20, 22-30,

30-40 at beam energies E=42, 92, 137 MeV/nucl. respectively, Fig. 3.7. The above-mentioned microcanonical model (FREESCO) does not yield a minimum of Σ at the same time for light fragments (p-α) and intermediate fragments (Li-N). Fig. 3.6-8. While the light fragments show a relatively high entropy according to the Σ analysis, the intermediate fragments have an entropy value by almost one unit smaller [CF87].

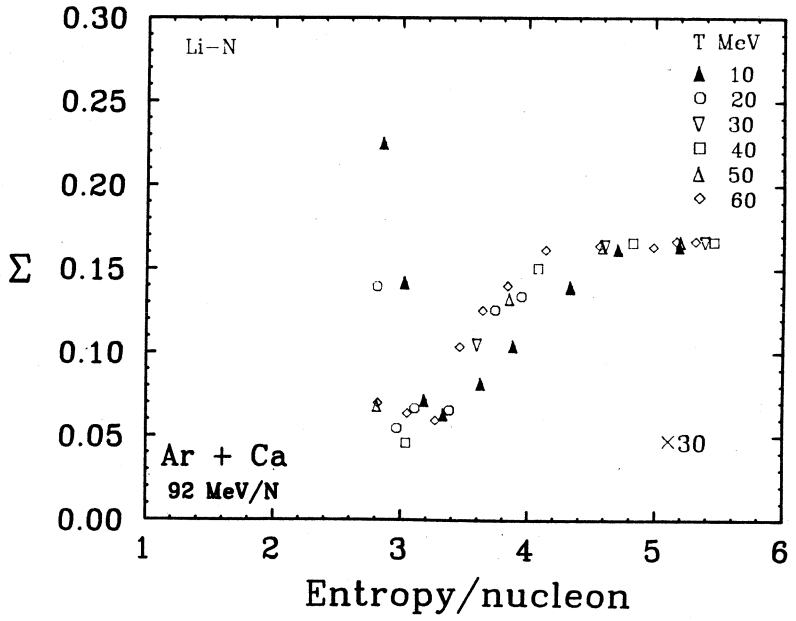

Fig. 3.8 Plot of Σ for heavier emitted fragments for the same reaction that is shown in Fig. 3.6. The heavy fragments show a lower entropy. From [CF87].

This indicates that the above model cannot yield satisfactory results at lower energies, and other effects like the nuclear liquid-gas phase transition [Cs85], microcanonical statistics, attractive and Coulomb interactions should be considered.

It is important to mention that the effects of microcanonical statistics become more important at low energies where the available excitation energy is strongly limited. A recent study [CF87b] shows that the relative yield of intermediate, A=10-15, fragments to the nucleons is suppressed by 30-60% in a small system of 28 nucleons, at T=10 MeV n=0.028 fm^{-3}. Fig. 3.9.

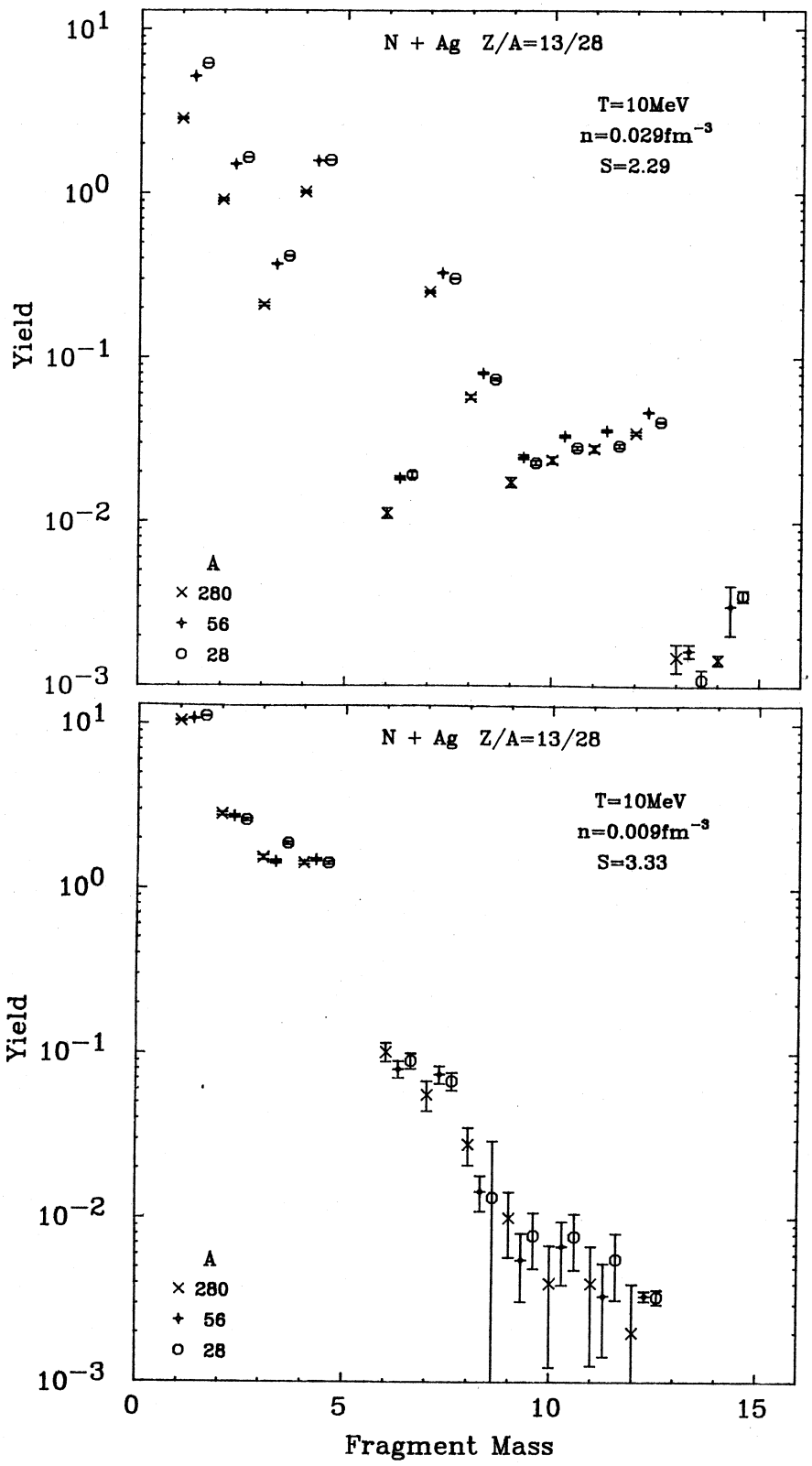

Fig. 3.9 Fragment mass yields depending on the size of the system and excitation energy calculated in the FREESCO microcnonical model [CF87].

Therefore at low energies and for small colliding nuclei, grand canonical statistics cannot yield accurate results. Also interactions and surface effects are not negligible anymore compared to the excitation energy.

3.4 Droplet and Bubble Formation

Let us first consider the surface effects. Suppose that in a central collision between heavy nuclei an intermediate state of high temperature and density is reached and that subsequently it undergoes an adiabatic expansion as discussed in previous section. Then, no matter what the entropy per baryon is, it will eventually intersect the Maxwell curve separating liquid and gas phases. See Fig. 1.2. What happens next depends on whether the system hits the Maxwell curve from the liquid side ($n>n_c$) or from the gas side ($n<n_c$). If from the liquid side, bubbles begin to form, and if from the gas side, droplets begin to form [Si83]. The initial formation of droplets or bubbles can be studied using statistical methods. For definiteness we shall consider the formation of droplets in a gas. Bubble formation is analogously studied by interchanging the liquid and gas labels.

The probability of droplet formation is estimated by calculating the change in the Gibbs free energy of the system when a droplet appears in the gas [LL54], [Re65]. The Gibbs free energy is the relevant one since the droplet and gas should be in kinetic equilibrium (equal pressures and temperatures) but not necessarily structural, or chemical,

equilibrium. Thus suppose that a spherical droplet containing A nucleons spontaneously forms in a gas consisting originally of a total number A+B nucleons.

$$G_{\text{no drop}} = \mu_G(A+B) \tag{3.17}$$

$$G_{\text{with drop}} = \mu_L A + \mu_G B + 4\pi R^2 \sigma_s + T\tau \ \ell n \ A \tag{3.18}$$

Here μ_G and μ_L are the nucleon chemical potentials in the gas and liquid phase respectively at pressure p and temperature T. The third term in eq. (3.18) is the surface free energy for a droplet of radius R and with surface tension $\sigma_s = \sigma_s(T)$. The last term in eq. (3.18) was introduced by Fisher [Fi67]. It takes into account the fact that the droplet surface closes on itself which reduces the total entropy associated with surface fluctuations. In mean field theories $\delta=1/3$ thus $\tau=7/3$.

The probability of formation of the droplet is proportional to $\exp(-\Delta G/T)$ where ΔG is the difference between eqs. (3.18) and (3.17). The yield of a fragment of mass A is

$$Y(A) = Y_o \exp\left[\frac{\mu_G-\mu_L}{T} A - \frac{4\pi r_o^2 \sigma_s}{T} A^{2/3} - \tau \ \ell n \ A\right]. \tag{3.19}$$

Here Y_o is a normalization constant and r_o is related to the droplet radius by $R=r_o A^{1/3}$ and to the density by $n_L^{-1}=4\pi \cdot r_o^3/3$. The importance of the surface effects was first observed by the Purdue-Fermilab group [FA82, MA82, HB84] and applied to high energy, 80-350 GeV, proton-nucleus reactions. Mass and charge distributions for A up to 30 were measured with higher precision than ever before possible because of the use of an in beam gas jet target. Arguments based on emulsion experiments [Ta77] and on temperature measurements suggested that these fragments come from a common thermalized source. The fragment mass distribution for a krypton target is shown in Fig. 3.10. It was noticed that a power law $A^{-2.65}$ fits the data better than an exponential $e^{-\alpha A}$.

The novel interpretation was that the target nucleus was almost instantaneously heated by the passage of the ultrarelativistic proton, and that subsequently the heated nucleus expanded in size until it passed through the critical point, $T=T$ and $n=n_c$, of the liquid-gas phase transition. At that point the distribution of droplets is

$$Y(A) = Y_0 \, A^{-\tau} \tag{3.20}$$

because in eq. (3.9) $\mu_G=\mu_L$ and $\sigma_s=0$ at the crtical point, so the volume and surface free energy terms vanish. There is no distinction between liquid and gas at the critical point, only long range fluctuations.

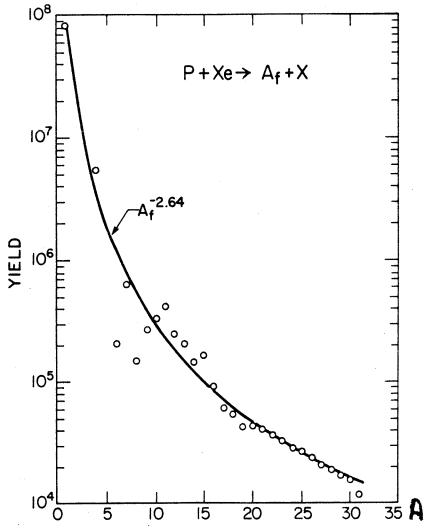

Fig. 3.10 Mass yield for 80-350 GeV protons on a gas jet Xenon target. From [FA82].

There are at least two difficulties with the above interpretation. First, why should one be so lucky to hit the critical point of nuclear matter accidentally with proton energies ranging from 80 to 350 GeV and with targets so different in size as krypton and xenon? Second, according to Fisher's version of the droplet model, $2<\tau<2.5$, whereas the data imply that $\tau = 2.65$, which is outside that range.

The above phenomenology was generalized to allow for the fact that one may not always be so lucky as to hit the critical point T_c, but that nevertheless one may get phase separation at some $T<T_c$ [Si83]. If the phases are in chemical equilibrium, $\mu_G = \mu_L$, then the usual Maxwell conditions apply. If so then from eq. (3.9)

$$Y(A) \propto A^{-\tau} \exp\left[-\frac{4\pi r_0^2 \sigma_s}{T} A^{2/3}\right] . \qquad (3.21)$$

For a finite range in A, say from 4 to 30, it is virtually impossible to distinguish between eqs. (3.20) and (3.21). A nonzero value of the surface tension $\sigma_s(T)$ can mimic an unphysically large value of τ ($\tau>2.5$). Fig. 3.11.

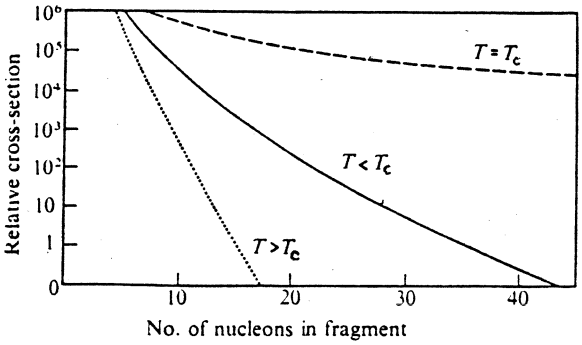

Fig. 3.11 Expectrd mass yields around the critical point. From [Si83].

The theoretically expected value of τ lies in a narrow range, being 2.33 in mean field approximation and about 2.2 in Wilson's renormalization group approach [Wi71]. Therefore, if one is able to determine T from the data, one ought to be able to infer $\sigma_s(T)$, which is an important property of nuclear matter.

A compilation of proton-nucleus and nucleus-nucleus data was made to test the hypothesis that the critical point could be located experimentally [PC84,Bo84,PC85]. The fragment mass distributions, generally in the range $10<A<30$, were fit with a power law for different experiments

$$Y(A) \propto A^{-\tau_{eff}} , \qquad (3.22)$$

and the apparent temperature of the fragments was estimted from the energy spectra at the same time. The effective exponent τ_{eff} is just a means of parametrizing the data. According to eq. (3.21) the yield should fall-off with a critical exponent $\tau_{eff}>\tau$ both above and below T_c.

The results of a compilation are shown in Fig. 3.12 [PC85]. There it is seen that initially τ_{eff} does decrease as T increases. There is then a gap in the data for 9 MeV < T < 12 MeV. If indeed there is a minimum in that range then it appears that T≈12 MeV and τ≈2. This would be quite an impressive result if it stands the test of time. Future

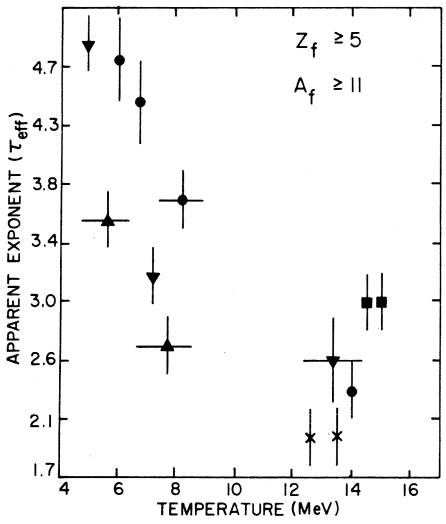

Fig. 3.12 The apparent exponent of the power law fit to the fragment mass yields as a function of the temperature T. The temperature was extracted from the energy spectra of the emitted particles. The points are representing a compilation of data from different colliding systems. From [PC85].

experiments hopefully will fill in the gap. However, it must be said that the data are also consistent with a monotonically decreasing τ_{eff} with increasing T. In particular there is no evidence for a rise in τ_{eff} if attention is focused only on a particular projectile-target combination.

It is interesting to mention that the liquid gas coexistence at the breakup could lead to a power law behaviour as it was suggested in [Cs85]. Really, calculating the fragment yields with the FREESCO code using two thermal sources with the parameters of a liquid and a gas phase in equilibrium with each other at T= 10 MeV temperature [FC85] leads to a power low type mass yield. Fig. 3.13.

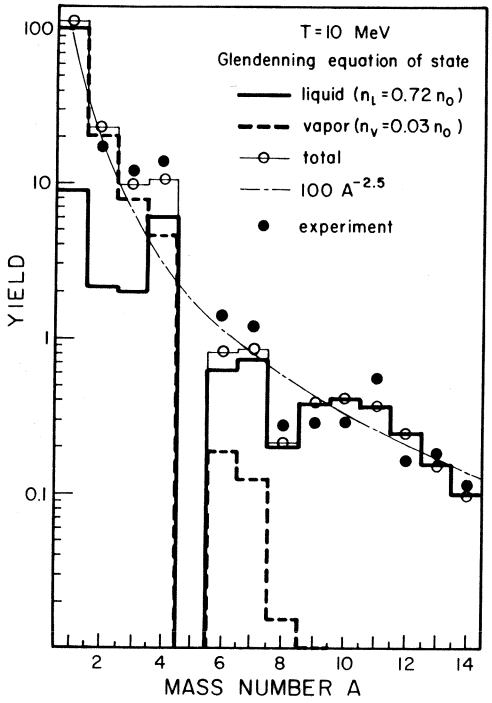

Fig. 3.13 Mass yields obtained from the disassenbly of of coexisting liquid (solid histogram) and gas (dashed histogram) phases at T= 10 MeV temperature. Open circles represent total calculated fragment yields with vapor fraction α = 1/2. Solid dots indicate experimental data Ar+Au at 42 MeV/nucl. From [FC85].

As we discussed in section 2, it is probable that the system does not reach the chemical equilibrium at the breakup: $\mu_G \neq \mu_L$. Then the first term in eq. (3.9) will not vanish. Thus in situation where $\mu_G > \mu_L$, eq. (3.19) predicts that the yield curve [GK84]

$$Y(A) = Y_0 \exp[aA - bA^{2/3} - \tau \ell nA] \tag{3.23}$$

has a minimum located at A_*. A_* is defined by the solution of

$$a - \frac{2}{3} bA_*^{-1/3} - \tau A_*^{-1} = 0,$$

shere $a=\mu_G-\mu_L>=0$. The droplet A_* at the minimum has the interpretation of being a critical droplet: smaller droplets are too small to overcome their relatively large surfaces, whereas larger droplets can and so will grow in an attempt to engulf the whole system.

A number of reactions were fit with the form (3.9) allowing $\mu_G \neq \mu_L$ [GK84]: Ne+Au at 250 and 2100 MeV per nucleon from the experiment of [WW83], and C+Au and C+Ag at 15 and 30 MeV per nucleon [CF83]. The most dramatic behavior is exhibited by the C+Au collisions where the yield has a minimum at Z=12 and then a rise by two orders of magnitude on either side. The droplet model is able to fit the data very nicely, in fact, with only one free parameter. The free parameter is the chemical potential difference between the phases or, equivalently, the degree of superheating of the system. It is very difficult to predict dynamically what this parameter should be, but at least it lies within the physically allowed region [GK84] (there is a limit to the amount a system may be superheated or supercooled).

Many of the phase space calculations may be capable of reproducing yield curves with U-shape as long as they include excited nuclei with charge up to at least Z=24. Thus, in the law of mass action, eq. (3.2), the volume term in the Boltzmann factor is $(\mu-\mu_0)A$. Here $\mu=\mu(n_{BU}, T)$ is determined by the overall density of the system at breakup. The $\mu_0 = \mu_0(n_0, T)$ is the chemical potential for nucleons inside a nucleus and at normal nuclear matter density n_0. As long as $n_{BU}<n_0$ it usually follows that $\mu > \mu_0$ and so the volume term in the exponential is positive. Therefore the droplet formula is essentially the same as the law of mass action with the important difference that in the former the droplets or excited clusters have an interface with nucleons at the same pressure and temperature and not the vacuum. This alters the surface free energy, and also means that the density of nucleons in a droplet n_L is less than normal density n_0, as assumed in the law of mass action.

3.5 Recent developments and prospects

The U-shaped mass spectrum in itself is not conclusive evidence for a phase transition. Numerous theoretical approaches yield a U-shaped spectra [GS82,XG86,BD85,BD85b,BB86,BB86c,BP86,BK85,BK86] and are able to fit the experimental results. Some of the important ingredients in these models are the Coulomb interaction, Fig. 3.14 [GS82], final decays

[FR83,St84,BB86] Fig. 3.15, and microcanonical effects [XG86,KR86, BD85, FR82]. The connection between percolation models and statistical fragmentation models has become a question of interest recently [BB86c, NB86]. The incorporation of attractive nuclear interactions into statistical fragmentation models is in progress [PS86].

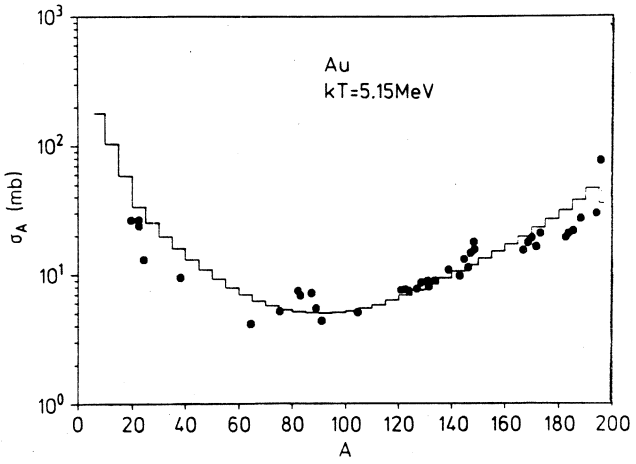

Fig. 3.14 Calculated mass-yield distribution for high energy p-Au reactions at T=5.15 MeV. The Coulomb effect leads to a U shaped mass yield [GS82].

To draw a conclusive opinion about the nuclear fragmentation models would be too premature now. One remark, however, is probably important to make: The connection between the nuclear fragmentation models and the nuclear EOS should be firmly established before a final conclusion about the nuclear liquid-gas phase transition can be drawn. So far the EOS underlying the statistical models was seldom calculated (apart from some simple cases [FR83]). In statistical fragmentation models the evaluation of the EOS is in principle possible although it may be very cumbersome. In percolation models the connection between the percolation parameter (like bond breaking probability) and the excitation energy and/or nucleon density is also undefined and so the

conclusion about an EOS is even further away. We may be confident, however, that in the near future a consistent nuclear EOS and fragmentation theory will arise form the large scale theoretical effort.

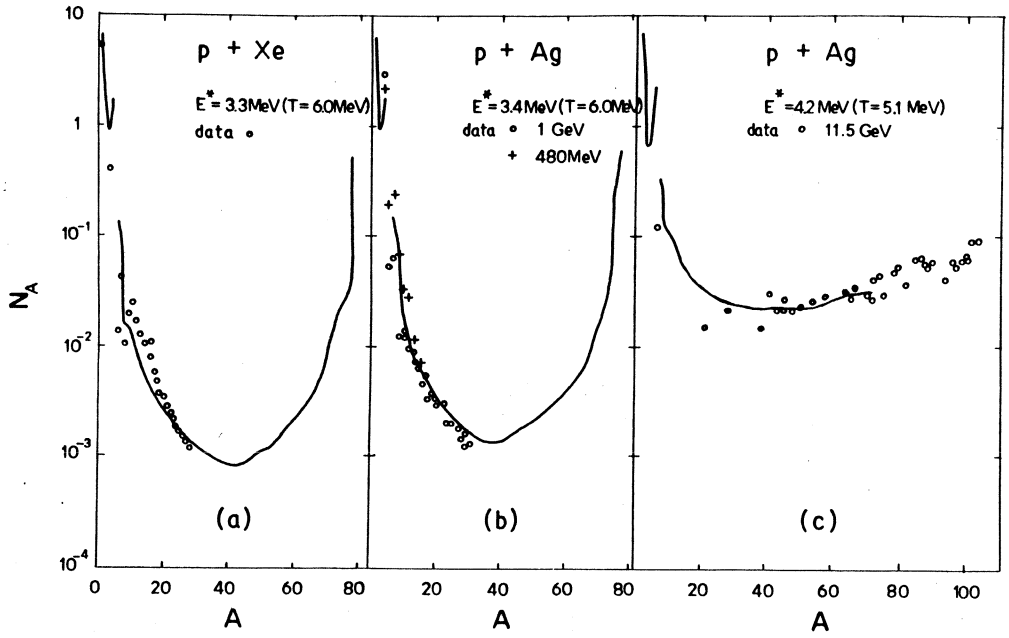

Fig 3.15 U-shape mass yields calculated in a statistical multifragmentation model for different proton induced reactions (curves). The calculation included the final decays of the primordial excited fragments. From [BB86c].

On the experimental side the problems are to separate central collisions and eliminate geometric effects arising in peripheral reactions. The most promising development in the near future will be the completion of a 4π detector at MSU with good mass and energy resolution. This will lead to a major step in understanding the mechanism of heavy ion reactions in the nuclear liquid gas phase transition region.

Acknowlwdgement

The author thanks Alex Brown and Wolfgang Bauer for the careful reading of the manuscript and for their comments.

4. References

AS86 J. Aichelin and H. Stocker, Phys. Lett., 176B (1986) 14.

AG78 A.A. Amsden, A.S. Goldhaber, F.H. Harlow and J.R. Nix, Phys. Rev. C17 (1978) 2080.

BB86 H.W. Barz, J.P. Bondorf, R. Donangelo, and H. Schulz, Phys. Lett. 169b (1986) 318.

BB86c H.W. Barz, J.P. Bondorf, R. Donangelo, I.N. Mishustin, and H. Schulz, Nucl. Phys. A448 (1986) 753.

BP86 W. Bauer, U. Post, D.R. Dean, ans U. Mosel, Nucl. Phys. A452 (1986) 699.

BB86b G.E. Beauvais, and D.H. Boal, Illinois Urbana rep. P/86/2/26

BC81 G. Bertsch and J. Cugnon, Phys. Rev. C24 (1981) 2514.

BS83 G. Bertsch and P.J. Siemens, Phys. Lett., 126B (1983) 9.

BK84b G. Bertsch, H. Kruse, S. Das Gupta, Phys. Rev. Lett. 54 (1984) 673.

Be71 H.A. Bethe, Ann. Rev. Nucl. Sci., 21 (1971) 93.

BK85 T. Biro, J. Knoll, Phys. Lett. 165B (1985) 256.

BK86 T. Biro, J. Knoll, and J. Reichert, Nucl. Phys. A459 (1986) 692.

BG76 J.P. Blaizot, D. Gogny and B. Grammaticos, Nucl. Phys. A265 (1976) 315.

Bo84 D.H. Boal, Phys. Rev. C30 (1984) 119, 749.

Bo84b D.H. Boal, Phys. Rev. C29 (1984) 967.

BP80 A.R. Bodmer, C.N. Panos, and A.D. McKellar, Phys. Rev. C22 (1980) 1025.

BD85 J. Bondorf, R. Donangelo, I.N. Mishustin, C.J. Petchik, H. Schulz, and K. Sneppen, Nucl. Phys. A 443 (1985) 321.

BD85b J. Bondorf, R. Donangelo, I.N. Mishustin, and Schulz, Nucl. Phys. A 444 (1985) 460.

CF83 C.B. Chitwood, D.J. Fields, C.K. Gelbke, W.G. Lynch, A.D. Panagiotou, M.B. Tsang, H. Utsunomiya and W.A. Friedman, Phys. Lett. 131B (1983) 289.

CB80 L.P. Csernai and H.W. Barz, Z. Phys. A296 (1980) 173.

CG81 L.P. Csernai and W. Greiner, Phys. Lett. 99B (1981) 85.

CL82 L.P. Csernai,I. Lovas, J. Maruhn, A. Rosenhauer, J.Zimanyi and W. Greiner, Phys. Rev. C26 (1982) 149.

CS83 L.P. Csernai,H. Stocker, P.R. Subramanian, G. Graebner, A. Rosenhauer, G. Buchwald, J.A. Maruhn and W. Greiner, Phys. Rev. C28 (1983) 2001.

CL83 L.P. Csernai and B. Lukacs, Phys. Lett. 132B (1983) 295.

Cs85 L.P. Csernai, Phys. Rev. Lett. 54 (1985) 639.

CK86 L.P. Csernai, and J. Kapusta, Phys. Rep. 131 (1986) 223.

CK86b L.P. Csernai, J.I. Kapusta, G. Fai, D. Hahn, J. Randrup, and H. Stocker, Phys. Rev. C submitted (1986) LBL-22183

CF86b L.P. Csernai, and G. Fai, Acta Phys. Hung. in press (1986)

CF87 L.P. Csernai, G. Fai, and G. Westfall, 1987 in preparation

CF87b L.P. Csernai, and G. Fai, 1987 in preparation

Cu80 J. Cugnon, Phys. Rev. C22 (1980) 1885.

CJ83 J. Cugnon and M. Jaminon, Phys. Lett. 123B (1983) 155.

Cu84 J. Cugnon, Phys. Lett. 135B (1984) 374.

CT83 M.W. Curtin, H. Toki and D.K. Scott, Phys. Lett. 123B (1983) 289.

Da79 P. Danielewicz, Nucl. Phys. A314 (1979) 465.

DG85 P. Danielewicz and M. Gyulassy, Phys. Rev. D31 (1985) 53.

Da78 S. Das Gupta, Phys. Rev. Lett. 41 (1978)1450.

DG86 S. Das Gupta, C. Gale, J. Gallego,H.H. Gan, and R.D.R. Raju Phys. Rev. C (1986) subm.

DG85 K. G. R. Doss, A. A. Gustafsson, H. H. Gutbrod, B. Kolb, H. Lohner, B. Ludewigt, A. M. Poskanzer, T. Renner, H. Riedesel, H. G. Ritter, A. Warwick and H. Wieman, Phys. Rev. C32 (1985) 116.

FR82 G. Fai and J. Randrup, Nucl. Phys. A381 (1982) 557.

FR83 G. Fai and J. Randrup, Nucl. Phys. A404 (1983) 551.

FR86 G. Fai and J. Randrup, Comp. Phys. Comm. subm., LBL-21537

FC85 G. Fai, L.P. Csernai, J. Randrup, and H. Stocker, Phys. Lett. 164B (1985) 265.

FA82 J.E. Finn, S. Agarval, A. Bujak, J. Chuang, L.J. Gutay, A.S. Hirsch, R.W. Minich, N.T. Porile, R.P. Scharenberg, B.C. Stringfellow and F.Turkot, Phys. Rev. Lett. 49 (1982) 1321.

Fi67 M.E. Fisher, Physics (N.Y.) 3 (1967) 255.

Fi71 M.E. Fisher, Proc. of Int. School of Physics, Enrico Fermi, Course LI, Critical Phenomena, edited by M.S. Green (Academic, New York, 1971).

GB86 C.Gale, G. Bertsch, and S. Das Gupta, Phys. Rev. (1986) subm.

GC86 N.K. Glendenning, L.P. Csernai, and J.I. Kapusta, Phys. Rev. C33 (1986) 1299.

GK84 A.L.Goodman, J.I. Kapusta and A.Z. Mekjian, Phys. Rev. C30 (1984) 851.

GK78 J. Gosset, J.I. Kapusta and G. Westfall, Phys. Rev. C18 (1978) 844.

Gr86 C. Grant, Phys. Rev. C34 (1986) 1950.

GS82 D.H.E. Gross, L. Satpathy, Meng Ta-chung and M. Satpathy, Z. Phys. A309 (1982) 41.

GI79 K.K. Gudima, H.Iwe and V. D. Toneev, J. Phys. G5 (1979) 229.

GT85 K.K. Gudima, V. D. Toneev, G.Ropke, and H. Schulz Phys. Rev. C32 (1985) 1605.

Gu45 E. A. Guggenheim; J. Chem. Phys. 12 (1945) 253.

GG84 H.A. Gustafsson, H.H. Gutbrod, B. Kolb, H. Lohner, B. Ludewigt, A.M. Poskanzer, T. Renner, H. Riedesel, H.G. Ritter, A. Warwick, F. Weik and H. Wieman, Phys. Rev. Lett. 52 (1984) 1590.

GG84b H.A. Gustafsson, H.H. Gutbrod, B. Kolb, H. Lohner, B. Ludewigt, A.M. Poskanzer, T. Renner, H. Riedesel, H.G. Ritter, A. Warwick, F. Weik and H. Wieman, Phys. Rev. Lett. 53 (1984) 544.

HB84 A.S. Hirsch, A.Bujak, J.E. Finn, L.J. Gutay, R.W.Minich, N.T. Porile, R.P. Scharenberg and B. Stringfellow, Phys. Rev. C29 (1984) 508.

JW83 B.V. Jacak, G.D. Westfall, C.K. Gelbke, L.H. Harwood, W.G. Lynch, D.K. Scott, H. Stocker, M.B. Tsang and T.J.M. Symons, Phys. Rev. Lett. 51 (1983) 1846.

JS84 B.V. Jacak, H. Stocker and G.D. Westfall, Phys. Rev. C29 (1984) 1744.

JF84 B.V. Jacak, D.Fox and G.D. Westfall, Phys. Rev. C31 (1985) 704.

JW87 B.V. Jacak, G.D. Westfall, G. Crawley, D. Fox, C.K. Gelbke, L.H. Harwood, B. E. Hasselquist, W.G. Lynch, D.K. Scott, H. Stocker, M.B. Tsang, G.Buchwald, and T.J.M. Symons, Subm. to Phys. Rev. C

JM84 H.R. Jaqaman, A.Z. Mekjian and L. Zamick, Phys. Rev. C29 (1984) 2076.

Ka81 J.I. Kapusta, Phys. Rev. C24 (1981) 2545.

Ka84 J.I. Kapusta, Phys. Rev. C29 (1984) 1735.

Ka84b J.I. Kapusta, Nucl. Phys.A418 (1984) 573c.

KR86 S.E. Koonin, and J. Randrup, LBL- 21165 rep. (1986)

KW76 S.B. Kaufman, M.W. Weisfield, E.P. Steinberg, B.D. Wilkins and D. Henderson, Phys. Rev. C14 (1976) 1121.

KJ85 H. Kruse, B. Jacak, and H. Stocker, Phys. Rev. Lett. 54 (1985) 289.

LL53 L.D. Landau and E.M. Lifshitz, Hydrodynamics (Nauka, Moscow, 1953).

LL54 L.D. Landau and E.M. Lifshitz, Statistical Physics (Nauka, Moscow, 1954).

LN79 M.C. Lemaire, S. Nagamiya, S. Schnetzer, H. Steiner and I. Tanihata, Phys. Lett. 85B (1979) 38.

LS84 J.A. Lopez and P.J. Siemens, Nucl. Phys. A431 (1984) 728.

Ma81 R. Malfliet, Nucl. Phys. A363 (1981) 429,456.

Ma84 R. Malfliet, Nucl. Phys. A420 (1984) 621.

Ma84b R. Malfliet, Phys. Rev. Lett. 53 (1984) 2386.

Me77 A.Z. Mekjian, Phys. Rev. Lett. 38 (1977) 640.

Me78 A.Z. Mekjian, Phys. Rev. C17 (1978) 1051.

MA82 R.W. Minich, S. Agarval, A. Bujak, J. Chuang, J.E. Finn, L.J. Gutay, A.S. Hirsch, N.T. Porile, R.P. Scharenberg, B.C. Stringfellow and F. Turkot, Phys. Lett. 118B (1982) 458.

MS83 I.N. Mishustin and L.M. Satarov, Yad. Fiz. 37 (1983) 894.

MH84 J.J. Molitoris, J.B. Hoffer, H. Kruse, and H. Stocker Phys. Rev. Lett. 53 (1984) 899.

MS85 J.J. Molitoris, and H. Stocker Phys. Rev. C32 (1985) 346.

MB84 D.J. Morrisey, W. Benenson, E. Kashy, B. Sherrill, A.D. Panagiotou, R.A. Blue, R.M. Ronningen, J. van der Plicht and H. Utsunomiya, Phys. Lett. 148B (1984) 423.

My76 W.D. Myers, Atomic Data Nucl. Data Tables 17 (1976) 411.

NB86 J. Nemet, M. Barranco, J. Debois, C. Ngo and E. Tomasi; Z. Phys. A325 (1986) 347; A323 (1986) 643.

Ni79 J.R. Nix, Prog. in Part. and Nucl. Phys., 2 (1979) 237.

PC84 A.D. Panagiotou, M.W. Curtin, H. Toki, D.K. Scott and P.J. Siemens, Phys. Rev. Lett, 52 (1984) 496.

PC85 A.D. Panagiotou, M.W. Curtin and D.K. Scott, Phys. Rev. C31 (1985) 55.

PS86 S. Pratt, P. Siemens, private comm.

RK81 J. Randrup and S.E. Koonin, Nucl. Phys. A356 (1981) 223.

RF82 J. Randrup and G. Fai, Phys. Lett. 115B (1982) 281.

Re65 F. Reif: Fundamentals of statistical and thermal physics (McGraw-Hill, 1965).

Re84 E.A. Remler, Phys. Lett. 145B (1984) 16.

RS83 G. Ropke, M. Schmidt, L. Munchow and H. Schulz, Nucl. Phys. A399 (1983) 587.

SY81 H. Sato and K. Yazaki, Phys. Lett. 98B (1981) 153.

SM74 W. Scheid, H. Muller and W. Greiner, Phys. Rev. Lett. 32 (1974) 741.

SK84 H.Schulz,B. Kampfer, H.W. Barz, G. Ropke and J. Bondorf, Phys. Lett. 147B (1984) 17.

SK79 P.J. Siemens and J.I. Kapusta, Phys. Rev. Lett. 43 (1979) 1486.

Si83 P.J. Siemens, Nature 305 (1983) 410.

SN80 A.J. Sierk and J.R. Nix, Phys. Rev. C22 (1980) 1920.

St71 H.E. Stanley: Introduction to phase transitions and critical phenomena (Oxford University Press 1971)

SB82 R. Stock, R. Bock, R. Brockmann, J.W. Harris, A. Sandoval, H.Strobele, K.L. Wolf, H.G. Pugh, L.S. Schroeder, M. Maier, R.E. Renfordt, A. Daca and M.E. Oritz, Phys. Rev. Lett. 49 (1982) 1236.

SB82b H. Stocker, G. Buchwald. L.P. Csernai,G. Graebner, J.A.Maruhn and W.Greiner, Nucl. Phys. A387 (1982) 205c.

SB83 H. Stocker, G. Buchwald, G. Graebner, P. Subramanian, J.A. Maruhn, W. Greiner, B.V. Jacak and G.D. Westfall, Nucl. Phys. A400 (1983) 63c.

St84 H. Stocker, J. Phys. G10 (1984) L111, and LBL preprint LBL -12302 (1981).

St84b H. Stocker, Nucl. Phys. A418 (1984) 587c.

SK84b B. Strack and J. Knoll, Z. Phys. A315 (1984) 249.

SC81 P.R.Subramanian, L.P. Csernai, H.Stocker, J.Maruhn, W.Greiner and H.Kruse, J. Phys. G7 (1981) L241.

Ta77 Y.P. Takovlev, Sov. J. Part. Nucl. 8 (1977) 106.

TG83 V.D. Toneev and K.K. Gudima, Nucl. Phys. A400 (1983) 173c.

VJ85 A. Vincenti, G. Jacucci and V.R. Pandharipande, Phys. Rev. C31 (1985) 1783.

WF85 C.J. Waddington and P.S. Freier, Phys. Rev. C31 (1985) 888.

Wa75 J. D. Walecka, Phys. Lett. 59B (1975) 109.

WW83 A.I. Warwick, H.H. Wieman, H.H. Gutbrod, M.R. Maier, J. Peter, H.G. Ritter, H. Stelzer, F. Weik, M.Freedman, D.J. Henderson, S.V. Kaufman, E.P. Steinberg and B.D. Wilkins, Phys. Rev. C27 (1983) 1083.

WG76 G.D. Westfall, J.Gosset, P.J. Johansen, A.M.Poskanzer, W.G.Meyer, H.H. Gutbrod, A. Sandoval and R. Stock, Phys. Rev. Lett. 37 (1976) 1202.

WY78 L. Wilets, Y. Yariv, and R. Chestnut, Nucl. Phys. A301 (1978) 359.

Wi71 K.G. Wilson, Phys. Rev. B4 (1971) 3174, ibid. 3184.

XG86 Z. Xiao-ze, D.H.E. Gross, X. Shu-yan, and Z. Yy-ming HMI-Berlin rep. (1986).